Review

Rodent Models and How They Define Potential Human Benefit: A Translational Review for Angelman Syndrome

Kelly M Knee [1*], **Edwin J Weeber** [1], **Niki Armstrong** [1], **Rachel E Stoub** [2], **Nicole A Copping** [1], **Barbara J Bailus** [2], **Yong-Hui Jiang** [3], **Elizabeth M Berry-Kravis** [4] **and Allyson Berent** [1]

[1]Foundation for Angelman Syndrome Therapeutics, San Antonio, TX, USA
[2]School of Pharmacy and Health Sciences, Keck Graduate Institute, Claremont, CA, USA.
[3]Department of Genetics, Yale School of Medicine, Yale University, New Haven, CT, USA.
[4]Department of Pediatrics, Neurological Sciences, and Biochemistry, Rush University Medical Center, Chicago, IL, USA.
Corresponding author: kelly.knee@cureangelman.org

Abstract

UBE3A silencing in primates consolidates around birth, leaving paternal UBE3A protein robustly expressed throughout early embryonic development. This developmental timing supports a largely postnatal pathogenesis in Angelman syndrome (AS) and provides a rationale for therapeutic benefit beyond infancy. Here we review AS genetics and imprinting biology, compare human and model-organism developmental timelines, and synthesize lessons from numerous AS mouse models, while simultaneously highlighting both their value for defining molecular mechanisms, biodistribution, and pharmacology, and their limits for predicting complex human outcomes. We summarize therapeutic strategies under evaluation (gene replacement, paternal allele unsilencing via antisense oligonucleotides or genome/epigenome editing, and hematopoietic stem-cell–based approaches) and emerging human trial results. Across modalities, data support the potential for meaningful rescue when UBE3A is restored postnatally across all ages, underscoring persistent circuit plasticity and the need for inclusive, age-spanning clinical trials, including newborn to adult ages, guided by rigorous biomarkers and translational endpoints.

Introduction

Neurodevelopmental disorders (NDDs) are distinct from traditional neurologic disorders in both etiology and progression, emerging primarily from disruptions in brain development rather than progressive degeneration. While neurologic disorders often arise later in life and involve specific regional or systemic pathology (e.g., epilepsy, stroke, or neurodegeneration), NDDs result from early-life perturbations to neurodevelopmental processes such as neuronal proliferation, migration, synaptogenesis, and circuit refinement. Within the heterogeneous spectrum of

NDDs, a critical distinction can be drawn between those with prenatal origins and those driven by postnatal insults. Prenatal NDDs are often more severe and less reversible (Knudsen 2004; Parenti et al. 2020) and may arise from early disturbances in maternal health or physiology, environmental exposures, or in utero stress and genetic disorders that impact early brain formation (Lutter et al. 2013; Grandjean et al. 2014; Bronson et al. 2016). These disruptions interfere with critical neurodevelopmental events, including cortical layering and axon pathfinding, potentially leading to structural and functional brain abnormalities that persist throughout life. Consequently, prenatal-derived NDDs often present with more global and intractable impairments and must be addressed by therapeutic strategies that require intervention during, or shortly after, gestation (Thomason et al. 2021; Thomason et al. 2024; Crider et al. 2022). In contrast, postnatal-derived NDDs typically reflect disruptions to experience-dependent plasticity or synaptogenesis/pruning and functional maturation. Though they may involve the same genetic risks or environmental factors as prenatal NDDs, their later onset likely provides a wider window for therapeutic intervention. Many early-life factors can interfere with brain plasticity and connectivity, shaping behavior over time (Rauh and Margolis 2016; Hensch 2005; Hensch et al. 2005; Thomason et al. 2024). Because of the brain's continued adaptability after birth, postnatal NDDs may be more responsive to treatment during extended developmental periods.

Angelman Syndrome as a model NDD

Angelman syndrome (AS) is a rare (~1:15,000) neurogenetic, developmental disorder caused by the loss of ubiquitin ligase E3A (*UBE3A*) gene expression in the brain (Kishino et al. 1997; Matsuura et al. 1997; Wagstaff et al. 1992). Individuals living with AS typically present with seizures, developmental delay, motor dysfunction, a uniquely happy demeanor, speech impairment, intellectual disabilities, and sleep abnormalities (Wagstaff et al. 1992; Margolis et al. 2015). While some symptoms of AS may begin in early infancy (e.g. feeding challenges), developmental delay onset is typically reported between 3-6 months, with seizures generally being reported at approximately 1-2 years (Williams et al. 2010). Genetic confirmation of the disorder generally occurs once symptoms have begun, with the improved availability of genetic testing meaning a conclusive diagnosis is commonly made at 1-2 years old (Sadhwani et al. 2024; Sadhwani et al. 2023; Khan et al. 2019). Despite the severe and challenging neurologic symptoms associated with AS, currently, there are no approved disease-modifying therapeutics, resulting in a significant clinical unmet need (Wheeler at al. 2017).

The ubiquitin ligase E3A (*UBE3A*) gene, located in the chromosomal region 15q11.2-13, is biallelically expressed throughout the body, but is only expressed from the maternal allele in neurons due to a process called brain-specific genomic imprinting (Rougeulle et al. 1998; Albrecht et al. 1997). Imprinting is a gene regulatory process occurring in a subset of genes, wherein genes from a specific parent-of-origin are epigenetically silenced or expressed. Within the 15q11.2-q13 region, a cluster of genes is regulated by a bipartite imprinting center comprised of two regulatory elements upstream of *UBE3A*, the Angelman syndrome imprinting center (AS-IC) and Prader-Willi syndrome imprinting center (PWS-IC), that determine the parent-of-origin expression. Several genes within this region have been linked to NDDs, including the *UBE3A* gene, which, when deficient, is associated with AS (Matsuura et al. 1997; Kishino et al. 1997). In neurons, paternal *UBE3A* is silenced due to a long non-coding RNA called the *UBE3A*-antisense RNA transcript (*UBE3A-ATS*) that initiates at the *SNRPN* promotor (Meng et al. 2012; Rougeulle et al. 1998). Alternatively, on the paternal allele, the PWS-IC remains unmethylated allowing for the initiation of *UBE3A-ATS* that is believed to block the transcription of the paternal *UBE3A* gene (Meng et al. 2012).

The *UBE3A* gene spans ~120 kb and encodes for a 100 kDa ubiquitin protein ligase E3A, an enzyme that acts both as a part of the ubiquitin-proteasome system designed for proteolysis of targeted proteins and as a non-specific transcriptional coactivator of nuclear hormone receptors (Yang et al. 2025). UBE3A belongs to the HECT (homologous to E6-AP COOH-terminus) family of enzymes that act to flag proteins for proteasomal degradation via the transfer of a ubiquitin tag (Scheffner et al. 1995; Bernassola et al. 2008; Mishra et al. 2008). Many mutations, including
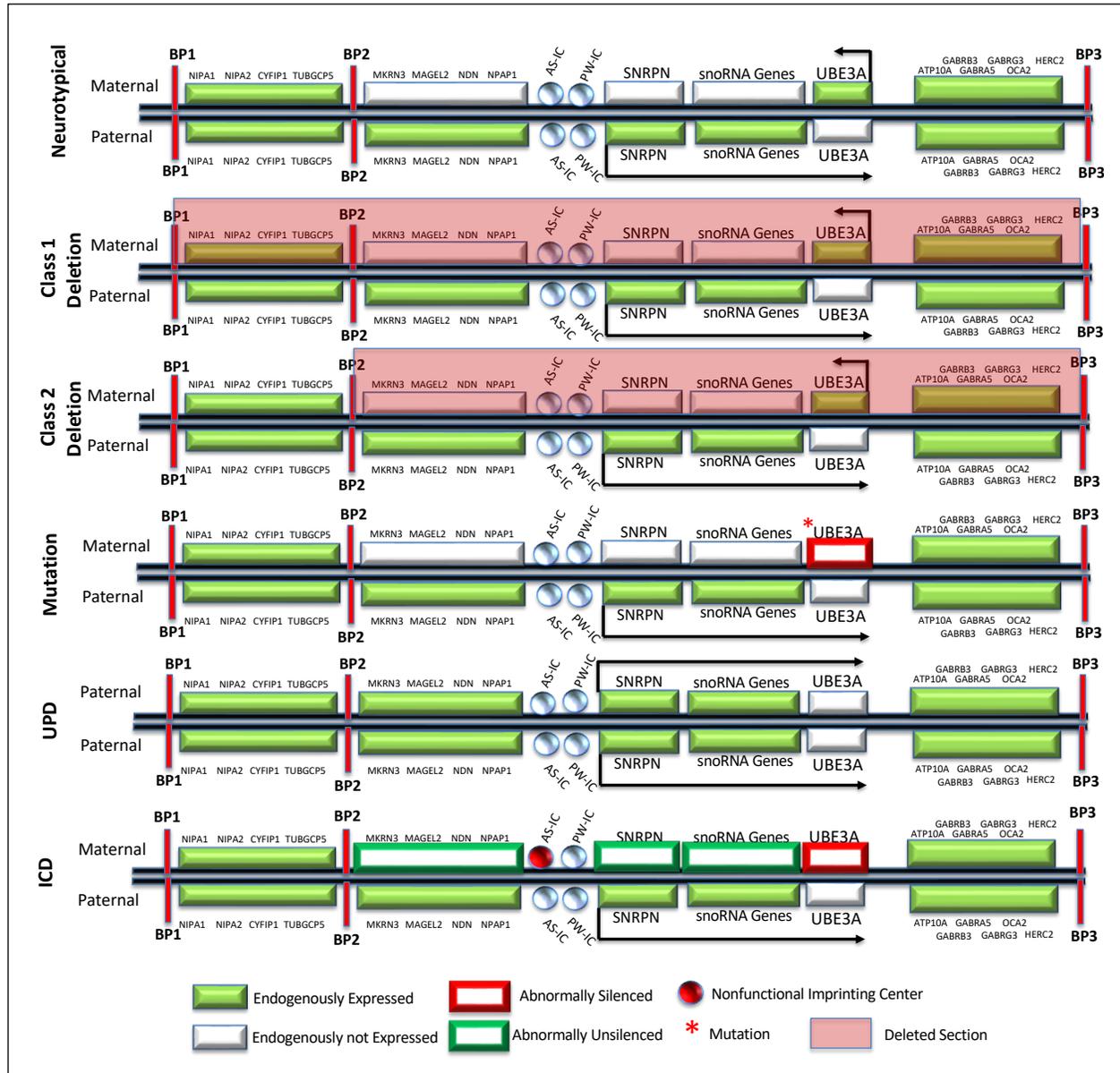
Figure 1. Human chromosome 15q11-13 and the genetic causes of Angelman syndrome.
Neurotypical: Some genes show mono-allelic expression due to genomic imprinting, meaning one parental copy is expressed (endogenously expressed) and one copy is naturally silent (endogenously not expressed). Loss of maternal *UBE3A* can occur by: **(1)** Deletions include Del1/Del2 (class 1/2, characteristic breakpoints). **(2)** Mutation (* maternal UBE3A mutations), including truncating changes that stop or severely shorten the protein and missense or small in-frame changes that alter a single amino acid or a short stretch of the protein, resulting in reduced or abolished UBE3A function. **(3)** UPD (paternal uniparental disomy) in which both chromosome 15 copies are paternal, causing absent *UBE3A* and overexpression of *MKRN3 to snoRNA* genes. **(4)** ICD (imprinting center defects) occurs when maternal *UBE3A* fails to turn on, sometimes due to mutation or deletion of the AS-IC. ICD is often accompanied by overexpression of paternally expressed genes in 15q11–q13 (*MKRN3–SNRPN*) (Abnormally unsilenced).

missense, frameshift, and nonsense mutations observed in AS affect the C-terminal catalytic domain of UBE3A (Tomaic et al. 2015; Christian et al. 1999). Additionally, while point mutations are detected throughout the entire coding region of *UBE3A*, many clusters frequent that same catalytic region, ultimately affecting the ligase activity of UBE3A (Cooper et al. 2004). Interestingly, the function of UBE3A as a non-specific transcriptional coactivator is independent of its role in the ubiquitin-proteasome system where mutations affecting the ligase activity do not change the coactivator activity, suggesting the symptoms of AS are likely due to the ligase activity where, when function is disrupted, unnecessary proteins build up and affect neural development and function (Nawaz et al. 1999).

There are several molecular mechanisms that can lead to the loss of functional *UBE3A* expression in the brain, resulting in AS (Figure 1). The most prevalent genetic subtype, accounting for 60-80% of the AS population, are *de novo* interstitial deletions within the 15q11-13 region on the maternal chromosome. These are deletions that are traditionally subclassified as Class 1, spanning breakpoint (BP) 1 to BP3 (~6 MB) or Class 2 spanning BP2 to BP3 (~5.0 MB), including many genes along the 15q11-13 region, including *UBE3A*. Individuals with this genotype generally have greater clinical challenges across all of the functional domains, including seizures, sleep, cognitive function, communication ability, motor ability, and daily living skills (Lossie et al. 2001; Gentile et al. 2010; Keute et al. 2021), likely due to the loss of the additional genes outside of *UBE3A*. AS can also be caused by mutations occurring in the maternal *UBE3A* gene, which account for approximately 10% of all AS individuals (Sadhwani 2024) (Figure 1). The discovery of point mutations and small intragenic deletions or insertions (indels), specifically disrupting maternal *UBE3A* expression and function, helped to establish the causal role of *UBE3A* in Angelman syndrome (Kishino et al. 1997; Matsuura et al. 1997). Imprinting defects (ICD), where the paternal allele methylation patterns are repeated on the maternal allele, and paternal uniparental disomy (UPD), where two paternal copies of *UBE3A* are inherited resulting in bi-allelic silencing of this region, are less common causes of AS and account for ~5-10% and 10% of cases, respectively (Figure 1) (Sadhwani et al. 2024). These genotypes result in a loss of neuronally expressed UBE3A protein, similar to the other genotypes, with an overall loss of function and clinical features of AS. Finally, there are also reported mosaic individuals living with AS (Baker et al. 2022; Buiting et al. 1998; Fairbrother et al. 2015; Nazlican et al. 2004) where most, but not all, cells lack expression of maternal *UBE3A*.

Individuals with mosaic maternal *UBE3A* expression often present with a significantly milder phenotype (Carson et al. 2019; Punatar et al. 2022) and may be precluded from typical diagnostic testing due to an atypical clinical presentation or the limited sensitivity of current detection technology. Individuals with mosaicism have been documented to have between 1-40% of cells expressing maternal *UBE3A* peripherally (Nazlican et al. 2004). Based on these estimates, the clinical severity seems to be positively correlated with peripheral expression, suggesting that a small number of neurons expressing *UBE3A* in the brain could result in a milder phenotype than that of the majority of the AS population (97-99%) experiencing 100% neuronal *UBE3A* deficiency. This includes individuals with as low as 1-5% of cells expressing maternal *UBE3A* who can speak words or sentences, have minimal to no gait disturbances, ataxia, or seizures (Fairbrother et al. 2015; Punatar et al. 2022; Nazlican et al. 2004). In most of the reports of mosaic individuals, detection of maternal expression above 40% has not been documented, suggesting that those individuals are either minimally impacted or asymptomatic and not subject to genetic testing.

As discussed previously, AS is increasingly recognized as a postnatal NDD, with hallmark features emerging after birth. At the time of delivery, infants with AS typically appear phenotypically normal, lacking distinctive dysmorphic features, no known brain anatomic abnormalities, and no neurologic abnormalities that would prompt immediate evaluation. Fryburg et al. (1991) and Zori et al. (1992) both describe that prenatal histories, delivery, and early neonatal courses are generally unremarkable, with clinical signs such as hypotonia, feeding difficulties, and developmental delay only becoming apparent within the first few weeks to years of life (Fryburg et al. 1991; Zori et al. 1992). However, there are reported clinical observations of early post-natal feeding difficulties, in particular problems coordinating sucking and swallowing (Williams et al. 2010). The full constellation of AS symptoms, including severe speech impairment, ataxia, epilepsy, and behavioral phenotypes, tends to emerge gradually over the first few years as milestones of typical neurodevelopment are missed. A more recent case report by Dang et al. (2023) further emphasized this point by illustrating how identification of atypical and subtle early signs, when recognized, can enable earlier diagnosis, though such cases remain the exception (Dang et al. 2023). Collectively, these findings highlight that the postnatal onset of symptoms, coupled with a typical appearance and normal brain structure, significantly contributes to delayed clinical recognition of AS during infancy and supports the assertion that AS is associated with potentially normal prenatal brain development.

These observations correlate with recent work by the Philpot laboratory that mapped *UBE3A* expression and *UBE3A-ATS* dynamics in the developing rhesus macaque brain. Using developmental time points spanning early gestation (gestation day (GD) 48) through late gestation (GD151) and into postnatal life, the study revealed that UBE3A protein is widely expressed prenatally across neocortical, hippocampal, and cerebellar regions, whereas *UBE3A-ATS* emerges progressively during mid-gestation (Gonzalez Ramirez et al. 2024). Specifically, *UBE3A-ATS* becomes detectable between GD48 and GD100, coinciding with cortical layer maturation, suggesting the onset of paternal allele silencing occurs before birth in primates. By late gestation, *UBE3A-ATS* is seen across cortical neurons, and postnatally this silencing pattern persists, with *UBE3A-ATS* expression restricted to neurons and absent in astrocytes. While the *UBE3A-ATS* is detected in late gestation, the extent of the ATS influence on paternal *UBE3A* expression, or brain region specificity, remains unknown. However, these data suggest that *UBE3A* silencing is primarily a postnatal event, which is supportive of the categorization of Angelman syndrome as a postnatal neurodevelopmental disorder.

Considering the distinction between prenatal and postnatal NDDs, Angelman syndrome (AS) provides a compelling example of a condition for which postnatal intervention may provide a meaningful benefit, and the fluidity of a critical age window of clinically meaningful benefit in the human brain should be strongly considered. Although AS has a genetic origin, it does not exhibit the irreversible structural brain malformations often associated with other severe prenatal NDDs. Instead, evidence from multiple studies in well-characterized animal models, as well as emerging clinical trial data in humans, suggests that functional deficits in AS may be significantly impacted even when intervention occurs postnatally, even into adulthood. Ideally, prenatal intervention would have the potential to address neuronal dysfunction before paternal *UBE3A* silencing, avoiding the development of any symptoms postnatally. However, there is abundant evidence that the prospect for potential meaningful benefit with postnatal treatment is strong.

Understanding the potential of therapeutic interventions to impact AS requires an understanding of the strengths and limitations of commonly used pre-clinical models and the differences between human and rodent brain development. This article will review the use of animal models in AS as critical tools for demonstrating proof of concept and prospects for benefit for various therapeutic modalities. These tools should be used as a mechanism for supporting potential efficacy, considering many variables, one being age, and another being the complexity of species. These models provide a tractable system for studying gene-dosage sensitivity, circuit plasticity, and the potential reversibility of behavioral phenotypes at different time points, with different anatomical targets and routes of administration. By leveraging the temporal and mechanistic benefits represented by these models, researchers have gained a general understanding of the efficacy parameters, biodistribution, pharmacokinetics, and translational potential of emerging therapeutic strategies for this population. However, it is important to recognize that a meaningful improvement in symptoms impacting the lives of individuals and their caregivers living with Angelman syndrome from a therapeutic intervention can be nuanced, and a complete reversal of all symptoms, albeit the ultimate goal, is not necessarily the only benchmark. Thus, expectations for the timing and magnitude of benefit in humans should reflect the greater complexity and far longer learning trajectory of the human brain relative to the mouse.

Developmental Windows in Model Animals in Relation to Humans:

Understanding the developmental trajectory of mice vs. humans is critical, both for contextualizing research done in model animals, and for drug discovery and development. The most common vertebrate model species, mice, have a similar progression of neurodevelopmental processes to humans and non-human primates, albeit on a significantly compressed time scale with far less complexity (Table 1). While the basic sequence of neural maturation, synaptogenesis, and circuit refinement is broadly conserved across mammals, mice undergo these events over a significantly shorter timescale relative to humans, making comparisons of

the timing of therapeutic interventions incredibly challenging.

For example, many of the neurodevelopmental processes that occur prenatally in humans take place postnatally in mice (Semple et al. 2013; La Manno et al. 2021). The first three postnatal weeks (postnatal day (P)1-21) in the mouse correspond roughly to the late third trimester through the first year of human life. In mice, this period is needed for modeling early-life sensory, motor, and cognitive development. This corresponds with the emergence of reflexes and voluntary motor behavior (e.g., righting, grasping, locomotion) that occurs between P7 and P14. Early tactile input via whisker stimulation is essential for the structural organization of the barrel cortex by P5, which can be compared to the role of early tactile and proprioceptive input involved in human somatosensory maps during the prolonged neonatal period.

Finally, while mice lack a direct equivalent of human speech, neonatal ultrasonic vocalizations (USVs) offer a primitive model for early vocal-motor integration and social communication. Mouse pups begin to emit ultrasonic vocalizations (USVs) within the first few hours after birth, typically starting around P1 (Pranic et al. 2022; Caruso et al. 2022). These early vocalizations are most prominent between P3 and P12, with the structure and complexity of USVs changing in adulthood (post P21), yet vocalization in humans as a mode of early vocal-motor integration and social communication generally starts at approximately 2-4 months of age with cooing and squealing with first words generally occurring between 10 and 18 months of age (Kuhl et al. 1996; Werwach et al. 2021).

In mice, brain development is highly specialized to support rapid postnatal maturation and immediate survival in a predatory environment. As prey animals, mice undergo accelerated neurodevelopmental processes that prioritize sensory acuity, spatial navigation, and threat detection. These functions rely on the hippocampus and may explain why the relative volume of the rodent hippocampus is 7-10 times larger than humans. For mice, the size and fast development of the hippocampus facilitates the swift formation of spatial memory and contextual awareness, enabling them to recognize, avoid, and escape predators soon after birth (Semple et al. 2013; La Manno et al. 2021).

Development of the human brain is substantially more complex, and occurs during both the pre- and postnatal periods, with certain stages being sensitive to environmental influences. Human brain development is characterized by prolonged postnatal plasticity and neoteny, supporting extended learning, complex socialization, and cognitive flexibility rather than immediate survival responses. The human hippocampus develops more gradually within a context of caregiver dependency and enriched social environments. This significant difference in developmental focus and timing between humans and mice means that direct translation of neurobehaviors and developmental milestones in mouse models is of limited utility for understanding human neurodevelopmental timelines and adaptive priorities, and care must be taken when attempting to draw developmental parallels between the two species (Semple et al. 2013).

In humans throughout the first two years of life, there are specific developmental periods that allow for the proper formation of neural circuits and the refinement of various skills. A number of these periods can be correlated with AS symptomology, for example, primary sensory systems, language development, and motor development. During the first two years of life, the human brain undergoes maturation of its primary sensory systems, including vision, hearing, and somatosensation (Hadders-Algra 2018). Motor development during the first two years of life represents a foundational component of neurobehavioral maturation and is characterized by the rapid emergence and refinement of both gross and fine motor skills. This period coincides with substantial growth in the central and peripheral nervous systems, including processes such as myelination of corticospinal tracts, maturation of motor cortices, and the establishment of sensorimotor integration pathways. Finally, language acquisition in humans occurs over a long period of time, but the greatest growth is thought to be within a well-characterized period spanning from approximately six months to seven years of age, during which the brain demonstrates exceptional neuroplasticity in response to linguistic input (Hadders-Algra 2018).

These general developmental periods can be broken down further as they represent temporally sensitive periods during which the somatosensory, motor, and

speech systems exhibit refined neuroplasticity, rendering them especially receptive to experiential shaping (Dehaene-Lambertz et al. 2015). During these phases, the brain's rapid synaptogenesis, myelination, and pruning processes are tightly coupled with sensorimotor experiences and linguistic exposure. This allows for the necessary calibration of specific neural circuits underlying touch, voluntary motor activation, and phonological encoding (Dehaene-Lambertz et al. 2015).

These developments can be broadly correlated with similar milestones in mice or humans (Table 1); however, drawing strong parallels of such complexity or time periods between human and mouse brain development is challenging. The human brain continues to develop, mature, and acquire skills well into adulthood, with neuroplasticity being somewhat dependent on environmental conditions (Pauwels et al. 2018; Gooijers et al. 2024). The most striking example of brain plasticity in adulthood is observed in adults who experience ischemic stroke (Dabrowski et al. 2019), or traumatic brain injury (Zotey et al. 2023), in which skills lost to damage can be regained following cognitive, motor, and sensory retraining (Zotey et al. 2023).

There are also multiple examples of skill acquisition in adulthood in the absence of injury, including learning a new language, adopting new technology, and managing chronic disease (Reed et al. 2014; Moxley et al. 2022; Sharit et al. 2020). These common instances of skill acquisition in adults suggest that the human brain continues to adapt and change throughout life, and thus, the consideration that therapies for NDDs may only be effective if delivered to young children near or before birth may not be valid.

The challenge in the interpretation of mouse developmental milestones is compounded when considering AS. Angelman syndrome is represented with an incredibly heterogeneous symptomology that is counter to deprivation studies and acute interruption of specific developmental windows (Margolis et al. 2015; Buiting et al. 2016). As an example, the lack of speech is one of the most universal characteristics of AS. However, quantitative measurements of communication ability in AS patients show that language is acquired by AS patients, but verbalization is hindered (Pearson et al. 2019). This suggests that a

circuitry challenge is at least partially responsible for the lack of speech and not necessarily a disruption in a critical developmental period. There is no direct correlation to this possible circuitry challenge that can be reliably assessed in mice, past measurements of ultrasonic vocalization, which do not report on comprehension or acquisition of vocalization. Similar challenges exist for comparisons of fine and gross motor skills, cognition, and anxiety-like behaviors. Further, the individual models themselves have conditions and limitations that must be considered when interpreting data obtained for true human translation.

Despite species differences and challenges with model comparisons, the AS mouse models have proved invaluable for demonstrating proof of concept for potential AS therapeutics and have provided important information about the feasibility of various treatment modalities as a translational model for drug development. What has been most challenging is drawing any strong conclusions when assessing how they may relate to the timing and impact of specific interventions.

Weeber and colleagues demonstrated that expression of a mutant form of *CaMKII*, a critical synaptic plasticity protein, could rescue long-term potentiation (LTP) and memory deficits in adult *Ube3a*-deficient mice (van Woerden et al. 2007), even though this transgene is not expressed during prenatal brain development. This finding supports the suggestion that key synaptic and behavioral phenotypes in AS can potentially be restored postnatally, and what has been considered an early "critical developmental window" is perhaps wider, more dynamic, and far more complex in higher species than originally thought in the rodent. This postnatal rescue highlights the broader therapeutic relevance of understanding the timing of pathogenic mechanisms in NDDs, and all disorders should not be considered equal.

In AS, synaptic dysfunction and circuit-level abnormalities appear to arise not from primary prenatal architectural disruptions, but rather from later deficits in synaptic plasticity, learning, and memory. These features position AS within the subset of NDDs that retain substantial developmental plasticity and therefore may potentially be more responsive to therapeutic interventions during extended postnatal

periods. These translational implications are significant and should be kept in mind in the context of this review; if underlying circuit integrity remains sufficiently intact to respond to therapeutic modulation, AS may be strongly amenable to treatment at multiple stages postnatally, resulting in clinically meaningful impact to individuals living with the disorder.

Stage	Mouse	Human
Prenatal	0–2.9 weeks gestation (E0–E19/20)	0–40 weeks gestation
Neonatal	0–1 week postnatal (P0–P7)	0–4 weeks postnatal
Juvenile	~2–4 weeks (P14–P28)	~4 weeks–520 weeks (~10 y)
Adolescent	~4–8.6 weeks (P28–P60)	~520–988 weeks (~10–19 y)
Adult	≥8.6 weeks (≥P60)	≥1040 weeks (≥20 y)

Table 1. Mouse–human life stage comparison and notation.

E = embryonic day (mouse, from conception); P = postnatal day (mouse, from birth, P0). Stage labels: prenatal, neonatal (birth~4 weeks human; P0–P7 mouse), juvenile (~P14–P28 mouse), adolescent (~P28–P60 mouse; ~10–19 years human), adult (≥P60 mouse; ≥20 years human).

The Mouse Models: Features and Limitations

There have been several transgenic mouse models generated since the discovery of *UBE3A* as the genetic cause of AS, all of which demonstrate some features relevant to the phenotypes observed in individuals living with AS. The AS mouse models have been instrumental in elucidating the molecular and circuit-level mechanisms underlying this NDD, providing a platform for evaluating genetic disruptions and therapeutic interventions. Following the generation of the AS mouse models, behavioral assays were commonly used to probe functional domains relevant to human symptoms, such as social interaction, communication, learning and memory, motor coordination, seizures, and anxiety-like behaviors. These paradigms were selected to approximate core features of NDDs in general and AS specifically, rather than attempt to replicate specific human behaviors. However, the translation of mouse behavior to human phenotypes is inherently limited by species-specific differences in brain structure, cognitive capacity, and behavioral complexity. Simplified behavioral tasks often lack the nuance necessary to capture the multifaceted nature of human symptoms, and interpretation can be confounded by factors such

as motor deficits or sensory alterations. For example, severe motor defects or anxiety in a mouse model can create serious interpretation caveats when evaluating more complex cognitive tests, like the hidden platform water maze or associative fear conditioning. A summary of the battery of behavioral, cognitive, motor, and physical tests used to characterize phenotypes and probe phenotypic changes is shown in Table 2.

In the domain of cognition, learning, and memory, the novel object recognition test assesses recognition memory through spontaneous exploration, capitalizing on rodents' innate preference for novelty; this task predominantly engages the perirhinal cortex and hippocampus. Contextual and cued fear conditioning engage associative learning mechanisms, especially hippocampal, amygdala, and medial prefrontal cortical circuits, by pairing a neutral stimulus with an aversive event and measuring subsequent conditioned freezing responses. The Morris water maze provides a robust measure of spatial learning and memory, requiring hippocampus-dependent navigation to a hidden platform based on distal spatial cues. Similarly, the Y-maze assesses working memory and exploratory behavior via spontaneous alternation, implicating prefrontal cortical and hippocampal function.

Motor coordination and balance are evaluated through a range of assays targeting cerebellar, basal ganglia, and sensorimotor cortical pathways. The accelerating rotarod quantifies balance and motor learning by measuring latency to fall from a rotating rod, with contributions from the cerebellum, motor cortex, and striatum. DigiGait™ provides high-resolution gait dynamics through computerized treadmill analysis, sensitive to both gross and subtle motor impairments associated with dysfunction in corticospinal, cerebellar, and brainstem locomotor circuits. The open field test, although often interpreted in anxiety contexts, also yields information on general locomotion driven by basal ganglia and motor cortex integrity. Beam walking evaluates fine motor coordination and balance, particularly under narrow or irregular beam conditions, and depends on cerebellar, vestibular, and proprioceptive integration. Hindlimb clasping, while often associated with motor deficits linked to corticospinal tract and cerebellar dysfunction, may also be an indirect marker of neuro-

Category	Assay	What it Measures	Description	Phenotype in AS mice	Brain Region(s) Engaged,	Correlation with human AS phenotype
Motor	Rotarod	Balance, coordination, motor learning, muscle tone	Rotating tube that the mice must balance on for timed periods	AS mice lack balance and coordination, do not stay on the rotarod for as long as WT mice	Cerebellum, striatum, cortex	Individuals with AS have gross and fine motor challenges, including gait disturbance, ataxia, spasticity, uncoordinated movements, and compromised balance. Individuals with AS also have dysregulated sleep spindles, which impacts ability to acquire new motor skills. Angelman syndrome individuals have reduced muscle coordination and reduced fine motor skills resulting in reduced ability to steadily grip objects.
Motor	Open field	Exploratory behavior and movement ability	An enclosed area in which voluntary movement around the space is recorded	AS mice are less mobile and do not explore the open space as much as WT mice	Cerebellum, striatum, cortex	
Motor	Balance Beam	Balance, coordination, gross and fine motor skills	A thin rod the mouse is forced to walk across	AS mice take longer to cross and are more prone to falling than WT mice.	Cerebellum, striatum, cortex	
Motor	DigiGate™	Physical characteristics of stride length, width, and pressure distribution on foot and motor learning	Treadmill that records paw patterns and walking speed	AS mice have a different gait pattern in the hind or fore limbs compared to wildtype littermate controls	Cerebellum, striatum, cortex	
Motor	Nest Building	Natural drive to build a shelter from available materials representing innate behaviors as well as motor skills and cognition	Individually housed mice are given a pre-weighed amount of nesting material; After a set time, the amount of material that has not been used to build a nest is weighed	AS mice do not build complex nests, in many cases they appear unable to manipulate the material into a recognizable structure or nest	Hypothalamus and preoptic region	
Motor	Marble Burying	Used to assess repetitive burying behaviors and anxiety-like behaviors. Act of burying requires motor coordination.	The mouse is placed in an enclosed area with a set of exposed marbles; The mouse is observed for a fixed time and the number of buried and partially buried marbles are counted	AS mice on average bury fewer marbles than WT mice. This may be at least partially due to motor and coordination impairments AS mice display. The contribution of anxiety to the difference between AS and WT mice is likely minimal	Hippocampus, limbic system	
Motor	Grip Strength	Assesses muscle strength and motor deficits	Mice are made to grasp a metal rod equipped with a force gauge that measures the maximum force used to resist a counter force (pulling). A variation of the assay has mice induced to grip on to a wire grid, which is then inverted so the mouse is suspended in the air, and the time required for the mouse to fall is recorded	AS mice generally exhibit reduced grip strength, however the differences are variable and are highly dependent on animals age, weight, and strain background	Motor cortex, premotor cortex, supramarginal gyrus	
Motor	Hindlimb clasping	Assesses motor coordination and neurological impairment	Mice are suspended by their tails to observe the position of their hind limbs. Increased clasping is indicative of neurological impairment.	AS mice usually display severe hindlimb clasp and significant reduction in "splay" of their hindlimbs.	Cerebellum, basal ganglia, neocortex	
Learning and Memory	Novel Object Recognition	Exploratory behavior, memory, recognition of new items	An enclosed container in which the mouse is presented with a familiar object and a new object; Time mouse spends engaging with the novel object is recorded.	WT mice prefer exploring a novel object to a familiar one, AS mice show a similar preference for both familiar and novel objects	Hippocampus, cortex	AS individuals have cognitive delays. Individuals with AS have short attention spans. Memory, sleep, language and behavior are all delayed relative to neurotypically developing peers
Learning and Memory	Fear Conditioning	Association of a stimulus with an unpleasant sensation	A test in which a stimulus (e.g. a bell ringing) is followed by an unpleasant sensation (mild electrical shock); With training, mice learn to associate the first stimulus with the following sensation and react to the stimulus	AS mice are less reactive to stimulus than WT mice under identical conditioning regimens	Hippocampus, cortex	
Learning and Memory	Morris Water Maze	Exploratory behavior pattern recognition	A swimming pool with a hidden platform surrounded by specific pictures, mouse learns to associate the orientation of the pictures with the location of the platform and swims to the platform faster each time they are placed in the pool	AS mice take longer to find the hidden platform relative to WT mice with identical conditioning regimens.	Hippocampus, cortex	
Learning and Memory	Y-Maze	Spatial memory, short term memory	Animals are placed in a maze with three arms and their tendency to alternate between arms is recorded; A higher percentage of alternation indicates better memory	AS mice are less likely to alternate between arms relative to WT mice with identical conditioning regimens.	Hippocampus, prefrontal cortex.	
Behavior	Marble Burying	Used to assess repetitive burying behaviors and anxiety-like behaviors.	The mouse is placed in an enclosed area with a set of exposed marbles; The mouse is observed for a fixed time and the number of buried and partially buried marbles are counted	AS mice on average bury fewer marbles than WT mice. However, the contribution of anxiety to the difference between AS and WT mice is likely minimal, and the reduced burying activity can be attributed to motor coordination deficits in the AS mice.	Hippocampus, limbic system	AS individuals have challenges with fine and gross motor skills. Challenging behaviors are often observed in individuals with AS. Hyperactivity is commonly reported in individuals with AS AS individuals have challenges building or organizing a space, i.e. building a Lego set or cleaning up a room AS individuals may exhibit more risky behaviors, potentially not understanding safety risks
Behavior	Nest Building	Natural drive to build a shelter from available materials representing innate behaviors as well as motor skills and cognition.	Individually housed mice are given a pre-weighed amount of nesting material; After a set time, the amount of material that has not been used to build a nest is weighed	AS mice do not build complex nests, in many cases they appear unable to manipulate the material into a recognizable structure or nest	Hypothalamus and preoptic region	
Behavior	Light/Dark	Assesses exploratory behavior and anxiety behaviors	The mice are placed in a container that has a "light/open" side and a "Dark/enclosed" side. The test then records how many times the mouse enters the "light/open" side; Anxious or behaviorally delayed animals will spend less time in the light	AS mice spend less time exploring the light side of the enclosure than WT mice, however these results may be confounded by the decreased locomotion and exploration behaviors observed in AS mice	Amygdala and hippocampus	
Behavior	Forced Swim	Assesses depressive behavior, and can also be used to evaluate stress response	Mice are placed in a cylindrical tank from which they cannot escape; The time spent immobile vs. treading water/swimming is recorded; Longer periods of immobility vs activity indicate a depressive/stress state	AS mice have mobility deficits and this may be reflected in their ability to swim for long periods of time; Due to these confounding mobility issues the test is instead used to measure how stress affects behavior in AS mice and is not directly related to depressive behavior	Limbic system and cortex	
Developmental and Physical	Growth	Quantitative measurement of body weight and length	Mice are weighed and measured from birth to death	AS mice are be influenced by strain background, genetic model and sex; General trends have observed that AS mice start out smaller than their WT littermates but that as they age the mice become overweight	N/A	Angelman syndrome individuals can exhibit a failure to thrive, are smaller in stature on average than age-matched peers without AS, exhibit scoliosis, and can exhibit microcephaly.
Developmental and Physical	Microcephaly	Quantitative measurement of brain weight	Brains of mice are weighed at different developmental stages	AS mice exhibit reduced brain weight (microcephaly) when compared with WT mice of the same age. Brain weight differences become apparent as soon as P5 and is not related to overall body weight.	Whole Brain	
Sleep	Sleep	Assesses disturbances in normal sleep/wake cycles	Gross measurements can be made by monitoring behavior and sleep/wake patterns. EEG is used to observe disturbances in REM and NREM sleep patterns.	AS mice exhibit disrupted sleep patterns with shorter REM and NREM periods, reduced sleep pressure and altered circadian rhythms when compared to littermate controls.	Hypothalamus	AS individuals often have disrupted sleep patterns with more frequent sleep/wake cycles, reduced periods of REM and NREM, and hyperexcitability
Electroencephalography/ Seizures	EEG	Assesses electrical activity in the brain	Electrodes are implanted into the skull and capture electrical activity while the mice move freely	AS mice exhibit increased power in low-frequency delta and theta oscillations, spontaneous epileptiform discharges (polyspikes) and altered sleep patterns when compared to WT animals	Cortex, hippocampus	AS individuals display high amplitude delta and theta waves, mixed with epileptiform discharges that are significantly different from non-AS age-matched individuals. AS individuals often have seizures, including myoclonic, atonic, atypical absence, and generalized tonic-clonic seizures
Electroencephalography/ Seizures	Induced seizure	Assesses seizure susceptibility and epileptogenesis	Seizures are induced by exposure to chemical or auditory stimuli and subsequent seizure activity is recorded	AS mice demonstrate heightened susceptibility to seizures following stimuli	Cortex	

Table 2. Mouse testing reference. AS= Angelman syndrome, WT= wild type, EEG= Electroencephalography, REM= rapid eye movement, NREM= non-rapid eye movement

Model (year)	Genetic Lesion	Motor / Cognitive / Behavior	Seizure/EEG	Sleep
Jiang (1998)	*Ube3a* maternal null (m−/p+) due to exon 2 deletion	Exhibits ataxia and reduced coordination Impaired open field tasks Exhibits impaired nest building Deficiencies in forced swim Impaired marble burying tests Deficient in Rotarod and wire hang tasks Impaired in contextual fear conditioning, water maze and novel object recognition. Enhance nociception to mechanical and heat stimulation Adult Obesity Impaired long-term potentiation (LTP)	Susceptible to seizures (audiogenic, chemoconvulsant and handling-induced). Exhibits abnormal EEG patterns, including high-amplitude spike-wave discharges, elevated delta power, and altered cortical rhythms	Exhibits fragmented sleep, shortened total sleep duration, disrupted REM architecture, and dampened expression of core circadian genes in the suprachiasmatic nucleus
Jiang (2010)	~1.6 Mb deletion (*Ube3a–Gabrb3*)	Deficient in rotarod task Impairments in Morris water maze Impairment in contextual fear conditioning Exhibits elevated ultrasonic vocalizations and anxiety-like behaviors in light/dark box.	Exhibits spontaneous seizures and increased seizure susceptibility Exhibits abnormal EEG spike-wave discharges	Not reported
Miura (2002)	Exon-based maternal *Ube3a* mutation	Deficient in Rotarod and bar-crossing tasks Impairment in water maze Impairment in contextual fear conditioning	Exhibits abnormal EEG including intermittent spike-wave discharges of variable frequency	Not reported
Judson (2016)	Floxed exon 7 conditional *Ube3a* KO	Not reported	Exhibits GABA-ergic *Ube3a* dependent increased susceptibility to audiogenic induced seizures Exhibits abnormal EEG including elevated delta power and spontaneous epileptiform activity	Not reported
Silva-Santos (2015)	Intron5 STOP cassette	Deficient in Rotarod Impaired open field tasks Exhibits impaired nest building Deficiencies in forced swim Impaired marble burying tests	Increased susceptibility to audiogenic seizures	Not reported
Avagliano Trezza (2019)	GABAergic-specific *Ube3a* knockout	Deficient in Rotarod Impaired open field tasks Exhibits impaired nest building Deficiencies in forced swim Impaired marble burying tests	Exhibits shift in synaptic inhibition/excitation balance Increased susceptibility to seizures	Not reported
Lee (2023)	Novel *Ube3a* mutation	Not reported	Exhibits abnormal power spectral densities and altered EEG rhythms in the frontal and somatosensory cortices.	Exhibits selective reduction of REM sleep.
Jiang (2025)	~6 Mb deletion 15q11.1-q13.1	Deficient in Rotarod Impaired open field tasks Deficient in novel object recognition Impaired marble burying.	Exhibits spontaneous seizures Increased sensitivity to seizure induction Increased frequency and duration of spike trains relative to *Ube3a^{m−/p+}* animals (Jiang 1998)	Not reported
Syding (2022)	Deletion of entire mouse *Ube3a* gene	Deficient in rotarod task Altered gait with DigiGait analysis Reduced activity in open field test Impaired nest building	Details not described	Males exhibited increased latency to first corner visit and first lick during light/dark phases

Table 3. Summary of key phenotypes reported in AS mouse models. AS=Angelman Syndrome, LTP= long-term potentiation, EEG = Electroencephalography, REM = rapid eye movement.

-degeneration or heightened limbic system reactivity. Additionally, nest building, a goal-directed, ethologically relevant behavior, is often disrupted in models of motor dysfunction, motivational deficits, or social-cognitive impairment, implicating a broader network involving the prefrontal cortex, hippocampus, and hypothalamus.

In the assessment of anxiety-like behaviors, several paradigms are employed, though they are interpreted cautiously due to species-specific ethological factors. The open field test evaluates thigmotaxis, with reduced center exploration often taken as an index of anxiety and linked to activity in the amygdala and prefrontal cortex. The forced swim test, traditionally used to assess behavioral despair, can also reflect stress reactivity and is associated with activity in the anterior cingulate cortex, prefrontal cortex, and locus coeruleus. The marble burying task, thought to reflect repetitive or anxiety-related behavior, involves quantifying the number of marbles buried over a fixed period and may involve striatal, orbitofrontal, and amygdalar circuits.

Seizure propensity and electrophysiological abnormalities are critical in models with underlying hyperexcitability or synaptic dysregulation. Behavioral observation of spontaneous or induced seizures, often scored using Racine scales, provides a functional readout of seizure susceptibility, typically originating in hippocampal, entorhinal, or neocortical circuits. Concurrent or standalone EEG recordings offer objective, high-resolution data on interictal spikes, epileptiform activity, and broader network synchrony disruptions, forming an essential bridge between behavior and underlying circuit-level pathology involving thalamocortical and limbic networks.

Assessment of communication in mouse models is challenging; however, ultrasonic vocalizations

(USVs) have been utilized to observe deficits in communication in $Ube3a^{m-/p+}$ mice when compared to WT animals (Jiang et al. 2010). Ultrasonic vocalizations are used by mice to communicate for numerous reasons, including pup/parent interactions and interactions with potential mates, as well as during periods of distress. Recent work by Guoynes et al. demonstrated that male $Ube3a^{m-/p+}$ mice make fewer USVs than male WT mice during courtship, and that the spectral properties and complexity of the USVs were different in male $Ube3a^{m-/p+}$ animals relative to male WT animals (Guoynes et al. 2025). Similarly, $Ube3a^{m-/p+}$ mice produce fewer USVs during distress than their WT counterparts, and USV production during distress was not sex-linked (Guoynes et al. 2025). These data suggest that differences in USV can distinguish between $Ube3a^{m-/p+}$ and WT mice, however, the specific protocols used to do the assessments must be standardized to make accurate comparisons, and whether the observed changes in USV frequency and complexity can be impacted by treatment remains to be seen (Guoynes et al. 2025). In addition, USV cannot be considered a direct comparison to the lack of verbal development in individuals with AS, as USV does not report on comprehension or acquisition of vocalization.

The mouse models have been essential to gaining a greater understanding of AS, and the molecular mechanisms which drive phenotypic expression. However, as with many disease-model animals, specific phenotypes and the degree to which they manifest is highly dependent on both the way in which $Ube3a$ is removed or decreased, and the background mouse strain, making comparisons between the different models challenging. These challenges are compounded when attempting to compare the effects of different therapeutic interventions, as the observed efficacy may be significantly influenced not only by the model itself, but by the route of administration of the therapeutic, the overall biodistribution, the volume of drug given, the duration of time after treatment the phenotype is analyzed, and the age of the animal at the time of treatment and at the time of assessment. In addition, the methods, cohort sizes, and experience of the operators performing the behavioral tasks on the animals can influence the outcome of the comparisons. In this section, we present an overview of the most-utilized mouse models for therapeutic translation, including performance on key behavioral and cognitive tests (Table 3).

Ube3a maternal null mouse (Ube3a $^{m-/p+}$)

The $Ube3a^{m-/p+}$ mouse model, generated through maternal deletion of exon 2 of the $Ube3a$ gene (Jiang et al. 1998), serves as the prototypical preclinical model of AS due to its close recapitulation of the disorder's neurological and behavioral phenotypes and full loss of expression (Jiang et al. 1998; Buiting et al. 2016; Keute et al. 2021). Loss of maternal $UBE3A$ expression, with the paternal allele silenced via neuronal imprinting, results in global absence of Ube3a protein in neurons. These mice exhibit pronounced motor impairments, including ataxia, reduced coordination, and deficits on tasks such as rotarod and wire hang. Cognitive dysfunction is a central phenotype, with impairments in hippocampus-dependent learning and memory, including contextual fear conditioning and novel object recognition, linked to severely reduced long-term potentiation (LTP) (Jiang et al. 1998; Born et al. 2017) (Huie et al. 2024; Huie et al. 2025). At the molecular level, disruptions in key synaptic signaling pathways, including abnormal CaMKII activity (Weeber et al. 2003) and dysregulated MAPK signaling (Filonova et al. 2014) contribute to impaired plasticity and memory formation.

The model also displays seizure susceptibility, especially in juvenile animals, with audiogenic and handling-induced convulsions and abnormal EEG patterns, including high-amplitude spike-wave discharges, elevated delta power, and altered cortical rhythms (Sidorov et al. 2017; Dickinson et al. 2025). These electrophysiological features are modulated by genetic background, with certain strains exhibiting heightened severity (Frohlich et al. 2019). Behaviorally, $Ube3a^{m-/p+}$ mice show hypersociability, reduced social discrimination, and hyperactivity, paralleling aspects of the AS behavioral phenotype. Recent work has identified significant sleep and circadian disturbances in this model, including fragmented sleep, shortened total sleep duration, disrupted REM architecture, and dampened expression of core circadian genes in the suprachiasmatic nucleus (Copping et al. 2021). Together, these general phenotypic domains encompassing motor, cognitive, behavioral, epileptic,

electrophysiological, and circadian behavior underscore the utility of the $Ube3a^{m-/p+}$ AS mouse model as a comprehensive and translationally relevant tool for investigating AS pathophysiology and therapeutic intervention, overwhelmingly serving as the standard AS model for translational research in AS.

Large Deletion Models:

Three discrete large maternal deletion models of AS, described by Jiang et al. (2010), Syding et al. (2022), and Lu et al. (2023), were designed to more comprehensively recapitulate the genetic lesions seen in most AS patients who carry large deletions spanning the 15q11–q13 region (Jiang et al. 2010; Syding et al. 2022; Lu 2023). These models differ in the extent and specificity of the deleted regions but converge on a common strategy of removing the maternal *Ube3a* allele and additional neighboring genes. The Jiang et al. (2010) model was generated using Cre/loxP-mediated chromosome engineering to delete approximately 1.6 Mb on the maternal allele encompassing *Ube3a*, *Atp10a*, and *Gabrb3*, producing the $Ube3a–Gabrb3^{m-/p+}$ genotype (Jiang et al. 2010). These mice demonstrate robust motor impairments (e.g., rotarod performance deficits), spatial and associative learning impairments (Morris water maze, fear conditioning), and behavioral anomalies such as elevated ultrasonic vocalizations in pups and anxiety-like behavior in the light–dark box, suggesting altered social and emotional processing (Jiang et al. 2010). Critically, this model exhibits spontaneous seizures, abnormal EEG spike–wave discharges, and heightened seizure susceptibility. Importantly, this reflects more severe connectivity and electro-physiological phenotypes when compared to the single-gene *Ube3a* deletion model. Although sleep behavior was not directly assessed, EEG abnormalities imply disrupted cortical rhythms that may affect sleep regulation (Jiang et al. 2010).

The Syding et al. (2022) model (*Ube3a* genedel) introduces a deletion of only the Ube3a locus (~76 kb), from 5′ UTR to 3′ UTR, eliminating all known coding and regulatory elements of the *Ube3a* gene, without removing adjacent genes such as *Gabrb3* or *Atp10a* (Syding et al. 2022). While this model also results in maternal deficiency and absence of neuronal *Ube3a*, it isolates the contribution of *Ube3a* loss from effects due to neighboring genes. Phenotypically, these mice exhibit core AS–like phenotypes, including motor impairments, such as reduced performance on the rotarod and altered gait in DigiGait analysis, and behavioral hypoactivity in open-field exploration (Syding et al. 2022). These mice also show deficits in goal-directed behaviors, exemplified by impaired nest building, and cognitive inflexibility, demonstrated by poor performance in reversal learning tasks using the IntelliCage system. Circadian activity monitoring indicated disrupted activity rhythms as well. While not as close to the large deletion genotype found in patients with AS, this model does offer advantages over the Jiang et al. (1998) exon 2 null mutation mouse model (Syding et al. 2022). By removing the entire *Ube3a* locus, it eliminates all coding and regulatory regions, ensuring complete loss of gene function and avoiding potential confounds from residual transcripts or truncated protein products. This structural precision may enhance its utility for testing gene reactivation or replacement therapies, particularly those targeting *Ube3a-ATS* or promoter regions. Moreover, the model more closely mirrors the genomic architecture of large deletions observed in many AS patients, thereby increasing its translational relevance for preclinical therapeutic development for this genotype.

Recently, the Jiang lab generated a new large deletion mouse model with an even longer 6MB deletion. This model was designed to more closely recapitulate the entire deleted genomic region (15q11.1-13.1), common to a majority of AS patients, and is known as the AS-LD$^{m-/p+}$ model. This model has the expected deficiency of *Ube3a*, as well as haploinsufficiency of the biallelically expressed genes *Tubgcp5, Herc2, Cyfip1, Gabrg3, Gabra5, Gabrb3* and *Atp10a* (Lu 2023). The AS-LD$^{m-/p+}$ mice are fertile and have no apparent developmental deficits. Behavioral analysis of these animals in comparison to wild type littermates included neurological screening, open field, marble burying, rotarod, and the novel object recognition test. AS-LD$^{m-/p+}$ mice showed reduced total travel distance and increased center time compared to WT littermates tested at 3-4 and 7-8 weeks of age. On the rotarod, the AS-LD$^{m-/p+}$ mice have reduced latency in both accelerating and steady paradigm, during both the first testing section and re-tests. In the novel object recognition test, AS-LD$^{m-/p+}$ mice did not show strong preference to the novel object as WT suggesting

deficits in both short and long-term memory. Both $Ube3a^{m-/p+}$ and AS-LD$^{m-/p+}$ mice were tested and compared for Flurothyl-induced seizure at 5-6 months. Both $Ube3a^{m-/p+}$ and AS-LD$^{m-/p+}$ mice have shorter latency for myoclonic seizure and tonic seizure compared to WT (Lu 2023). However, the AS-LD$^{m-/p+}$ mice were more sensitive to seizure induction compared to the $Ube3a^{m-/p+}$ mice. EEG of AS-LD$^{m-/p+}$ mice show significant increases in both the frequency and duration of spike trains, when compared to $Ube3a^{m-/p+}$ mice of the same age. In addition, AS-LD$^{m-/p+}$ mice have displayed propensity for spontaneous seizures, which is not present in the $Ube3a^{m-/p+}$ model (Lu 2023).

GABAergic neuron-specific Ube3a deletion

The GABAergic neuron-specific $Ube3a$ deletion model ($Ube3a\ DGABA\ ^{m-/p+}$) developed by Judson et al. (Judson et al. 2016) and further characterized by Avagliano Trezza et al. (Avagliano Trezza et al. 2019) offer a unique cell-specific targeted approach aimed at dissecting the contribution of inhibitory interneuron dysfunction to AS pathophysiology. Both models employ Cre-loxP recombination to conditionally delete the maternal $Ube3a$ allele in GABAergic neurons using the GAD2-Cre driver line, thus allowing $Ube3a$ expression in excitatory neurons while selectively disrupting it in inhibitory circuits. The Judson model introduces loxP sites flanking exons 2 and 3, resulting in a frameshift and complete functional knockout of $Ube3a$ in targeted cells (Judson et al. 2016). In contrast, the Avagliano Trezza model deletes exons 5 and 6, producing a truncated transcript that enables interrogation of subcellular localization and nuclear-specific functions of $Ube3a$, such as transcriptional regulation and chromatin modification (Avagliano Trezza et al. 2019). Phenotypically, both models recapitulate key features of the AS behavioral and neurophysiological profile, including deficits in motor coordination, impairments in learning and memory, and heightened sociability and hyperactivity. Importantly, both models show increased seizure susceptibility, including enhanced audiogenic-induced seizures and spontaneous epileptiform activity. Electrophysiological recordings reveal elevated neocortical delta power and background rhythm disturbances. Although sleep phenotypes were not systematically assessed, the cortical hyperexcitability inferred from the EEG patterns suggests possible alterations in sleep-wake dynamics. While similar in production, the Judson et al. model emphasizes the role of GABAergic dysfunction in circuit excitability and seizure generation, and Avagliano Trezza et al. highlights nuclear compartmentalization of Ube3a's role in epigenetic regulation.

Ube3a C-terminal deletion model

The $Ube3a$ C-terminal deletion mouse model developed by Miura and Kishino et al. (2002) (Miura et al. 2002) represents a mechanistically distinct approach to modeling AS by inducing a DNA mutation that destabilized the resulting Ube3a protein. This model was generated through targeted deletion of a region encoding the C-terminal portion of $Ube3a$ specifically, exon 5 of the long isoform, which includes the HECT domain necessary for its E3 ubiquitin ligase activity, resulting in a truncated form of the protein. This mouse model design preserves aspects of the gene's transcriptional control and isoform regulation, while in turn modeling certain partial loss-of-function mutations observed in a subset of AS patients more accurately than complete null alleles (Miura et al. 2002).

Phenotypically, these mice also exhibit hallmark features of AS, including significant motor coordination deficits, impaired spatial and associative learning and memory, and abnormal social and exploratory behaviors. Importantly, EEG recordings reveal epileptiform abnormalities, such as intermittent 4–5 Hz spike-wave discharges, reflecting cortical hyperexcitability consistent with AS-related epilepsy (Miura et al. 2002). This model provides an alternative to full gene deletions, which is useful for investigation into the functional consequences of domain-specific Ube3a loss, offering insight into how specific mutations might differentially impact protein function, neuronal networks, and behavior. However, as a model for testing potential therapeutics, the presence of a non-functional Ube3a may confound the interpretation of data, suggesting this model may be better suited for answering mechanistic or molecular questions.

Ube3a Δe6/p+ mouse model

The $Ube3a\ \Delta e6/p+$ mouse model, developed by Lee et al., employs CRISPR/Cas9-mediated excision of exon 6 on the maternal allele of the $Ube3a$ gene (Lee et al.

Knee et al.

2023). This targeted deletion induces a frameshift and premature stop codon in exon 7, leading to rapid degradation of the mutant transcript and a profound reduction in Ube3a protein within neurons. Quantitative analyses confirmed that brain expression levels fall to a small fraction (2–17% of wild-type) by postnatal week six. By eliminating a substantial portion of the HECT domain and disrupting all functional isoforms of the protein, this model closely approximates a true loss-of-function scenario and offers a more complete molecular null model compared to earlier partial truncation models such as Miura and Kishino's exon 5-deleted line (Miura et al. 2002). Functionally, these mice exhibit a constellation of deficits that reflect core AS phenotypes, including poor motor coordination, hippocampal-dependent learning impairments, and altered synaptic plasticity. High-resolution EEG recordings reveal pathological electrophysiological signatures, such as increased delta power and abnormal cortical rhythms, alongside heightened seizure vulnerability (Lee et al. 2023). This model is also distinguished by its comprehensive assessment of sleep architecture that shows significant reductions in overall sleep duration, fewer sleep spindles, and increased sleep fragmentation. In general, this model is extremely consistent with both the original $Ube3a^{m-/p+}$ model (Jiang 1998) and the exon 5-deleted line (Miura 2002), with no apparent differences in major AS phenotypes.

CRE-loxPox Model:

The conditional *Ube3a* reinstatement model developed by Silva-Santos et al. represents an effort to dissect the developmental timing and cellular specificity of Ube3a function in an AS mouse model (Silva-Santos et al. 2015). In this model, a floxed transcriptional stop cassette was inserted upstream of exon 2 in the endogenous *Ube3a* gene, creating a Cre-dependent "off" allele (*Ube3a*^lox-stop) that silences maternal *Ube3a* expression. This silencing is reversible through tissue-specific or temporally regulated expression of Cre recombinase, enabling reinstatement of *Ube3a* in selected neural populations or at specific postnatal times to 75-90% of wild type *Ube3a* levels (Silva-Santos et al. 2015). Importantly, baseline maternal-deficient *Ube3a* lox-stop/p+ mice exhibit behavioral and electrophysiological phenotypes consistent with AS, including impaired rotarod performance, deficits in contextual fear

conditioning, novel object recognition, and elevated delta power in cortical EEG recordings. Quantification of protein restoration following CRE-mediated excision indicates that Ube3a levels can reach approximately 30–50% of wild-type levels in targeted brain regions, depending on the timing and efficiency of recombination. Behavioral rescue in this model was strongly dependent on the age at which *Ube3a* expression was restored; prenatal restoration resulted in the most robust rescue of AS phenotypes including behavioral and EEG abnormalities (Silva-Santos et al. 2015). Later restoration in animals in the juvenile stage resulted in more limited rescue of AS phenotypes, and restoration in the adult stage resulted in the least significant AS phenotypic rescue (Silva-Santos et al. 2015). The conditional design of this model also allows for cell-type–specific interrogation; for instance, restoring *Ube3a* in excitatory neurons alone is sufficient to ameliorate motor and cognitive deficits, highlighting the central role of glutamatergic dysfunction in AS pathogenesis (Table 4).

One aspect of the CRE-*loxP* model that differentiates it from other AS mouse models is the use of Tamoxifen to reactivate the *Ube3a* gene. Tamoxifen is a selective estrogen receptor modulator that has been associated with a wide range of systemic side effects that raise concerns for its use in translational applications (Silva-Santos et al. 2015). The effects of Tamoxifen on the central nervous system and on mouse behavior are well known, including reduced locomotor activity, heightened anxiety, and impaired social interactions (Li et al. 2020; Galvano et al. 2023). Considering that several of the relevant mouse behaviors measured in AS overlap with behaviors impacted by Tamoxifen, the interpretation of data obtained using the CRE-*loxP* model must consider the possible contribution of Tamoxifen to the overall results. This is particularly important when evaluating the efficacy of potential drug compounds on AS phenotypes. The CRE-*loxP* model may be best suited to study the molecular mechanism and the timing of phenotypic development in a mouse model of *Ube3a* deficiency, while an AS mouse model that mimics the human genotype, and is not dependent on the administration of a confounding compound, should be used for evaluating potential AS therapies, which may be easier in interpreting results of therapeutic intervention.

Caveats of Mouse Models and Common Phenotypic Assays:

Across these AS mouse models, the unifying genetic feature is the loss of functional maternal *Ube3a* expression in neurons, achieved through diverse genomic strategies that differ in scope, precision, and cell-type specificity. The canonical Jiang 1998 maternal null (*m–/p+*) model achieves complete neuronal loss of *Ube3a* via maternal exon 2 deletion, serving as the foundation for most subsequent designs, and is the most widely used model to date for translational research proof of concept studies in both academic laboratories and by industry. Broader chromosomal deletions, as in Jiang 2010 (~1.6 Mb spanning *Ube3a–Gabrb3*) or Lu 2023 (~6 Mb deletion spanning the main large deletion genes), not only remove the *Ube3a* gene but also the neighboring genes, potentially compounding phenotypes with effects from contiguous gene loss. Conceptually, the ~6Mb maternal deletion model is the most appropriate model for preclinical studies of a majority of humans living with AS because it includes a complete deficiency of *UBE3A* as well as haploinsufficiency of other biallelically expressed genes within the 15q11.2–q13 region (Lu et al. 2023). Many of these genes—such as *CYFIP1, NIPA1/2, HERC2, GABRB3, GABRA5, and GABRG3*—are known to play important roles in neuronal function. Clinical findings support the idea that haploinsufficiency of some of these genes, either individually or in combination, may modify the phenotypic effects of *UBE3A* deficiency. Thus, the 6 Mb deletion model presents an opportunity to investigate these mechanisms, in addition the loss of *Ube3a* expression, particularly given the limitations of studying them directly in humans.

While each of these models has been useful for elucidating AS mechanisms of different genotypes and genetic variations, they all carry several limitations that constrain their translational reliability. The background strain used to construct the individual animal models confers strain-specific variability, leading to large differences in seizure penetrance, learning deficits, and EEG abnormalities (Martinez et al. 2023). This strain dependence complicates reproducibility across laboratories and may mask or exaggerate drug or genetic therapy effects. Moreover, some AS-relevant symptoms, such as the full range of expressive language deficits, complex cognitive function, fine motor skill impairments, or complex social-communication behaviors, cannot be adequately modeled in mice, regardless of how closely they genetically mimic the human disorder. In addition, knowing that human neuronal development and neuroplasticity continue over decades, whereas in mice it continues over days to weeks, makes extrapolation of human function from mouse model data challenging.

The complexity of the available phenotypic assays also complicates the interpretation of mouse model data. As outlined in Table 2, there are numerous assays for motor and cognitive function, maladaptive behaviors, and physical development. The outcome of many of these assays is dependent on the protocol used to administer them, making direct comparisons between studies done by different groups challenging. There are, however, a few assays which are consistently performed by most groups, which seem to yield the most reliable and comparable results. To assess motor function changes, the Rotarod (which includes motor function and motor learning) and open field tests (which includes both motor function and anxiety-like behaviors) are preferable and generally considered the most reliable; To assess cognitive function, novel object recognition is considered a reliable test; and for anxiety-like behaviors the most commonly used tests are open field and marble burying. In addition, nest building is commonly used, and a reliable assessment of overall function as it is a semi-quantitative measurement of multiple parameters, including innate function and motor, cognitive and behavior phenotypes. In addition to the relatively subjective neurobehavioral assessments in AS mice that can be impacted by other factors, like body weight and stress, assessment of EEG spectral power (e.g. delta power) is considered one of the most objective assessments that is subject to change after effective therapeutic intervention.

While important tools, these AS animal models simplify the pathophysiology of AS in a way that is advantageous for mechanistic studies, but potentially less predictive of clinical outcomes across diverse and complicated neurobehavior in the human AS population, which may explain why one could expect different therapeutic effect size in different individuals with AS due to their unique variables.

Therapeutic Strategies for Treatment of AS

Currently, there are no approved disease modifying therapies for AS, however, there are multiple candidate therapeutics in various phases of clinical and pre-clinical development, most or all of which have utilized one or more of the AS mouse models discussed in the previous section for evaluation of their potential benefit. Disease model mice are useful for demonstrating possible efficacy, establishing pharmacokinetic/pharmacodynamic relationships, estimating biodistribution and cellular specificity, establishing a preferred route of administration, and defining an efficacious dose range. In the following section, we review how the AS model mice were used in the development of many of the current clinical candidates and, when available, how the emerging open-label human data from ongoing clinical trials does, or does not, correlate with AS mouse data.

Adeno-Associated Virus-Mediated Gene Replacement Therapy

One of the most extensively explored strategies for the treatment of monogenic NDDs involves gene replacement therapy, in which a functional or "corrected" copy of a disease-causing gene is introduced into target cells via a complementary DNA (cDNA) construct. In the context of AS, reintroducing *UBE3A* via cDNA represents a rational approach to restore protein expression and, potentially, physiological and behavioral function. Adeno-associated virus (AAV) vectors have emerged as a leading platform to support cDNA delivery to target cells due to their limited pathogenicity, relatively low immunogenicity, ability to mediate long-term transgene expression in post-mitotic cells, and the flexibility of serotype engineering to achieve cell-type or region-specific tropism (Wang et al. 2024). A variety of AAV serotypes and engineered or modified capsids have been developed to enhance transduction efficiency in the CNS, including serotypes such as AAV9, which have been shown to achieve transduction in neurons when delivered into the CSF by intracerebroventricular (ICV), intracisternal magna (ICM), or intrathecal (IT) routes of administration (Wang et al. 2024).

The use of AAV-mediated *UBE3A* cDNA replacement for AS involves several critical considerations. First,

UBE3A is expressed in multiple isoforms generated through alternative splicing and promoter usage. The choice of which isoform(s) to deliver affects physiological relevance, subcellular localization, and therapeutic effectiveness. Second, regulation of *UBE3A* dosage should be carefully considered—both insufficient and excessive expression of this E3 ligase have been linked to different NDDs, though overexpression of UBE3A has been associated with other genes in the region that are also overexpressed by 200-400%. Therefore, careful vector and transgene design and promoter selection are key to ensuring the optimal outcome. Third, because the paternal *UBE3A* allele is silenced specifically in neurons, while glial cells express both alleles, it is important to use neuron-specific promoters to ensure targeted expression is achieved. Finally, due to the pan neuronal *UBE3A* deficiency in AS, the need for diffuse brain biodistribution is critical leading to careful consideration of route of administration for an optimal outcome (Hinderer et al. 2014). Additionally, the timing of vector delivery may be a crucial factor in preclinical models, with interventions in mice occurring as early as P1 or at various later time points, which can have an impact on transduction efficiency to different CNS cell types (Dhungel et al. 2021). This section reviews preclinical studies using AAV-based *UBE3A* gene replacement in AS mouse models, with a focus on vector type, Isoform selection, expression control, spatial targeting, route of administration, dose given, age treated, and behavioral outcomes, including both neurobehavioral and electrophysiological assessments, when available. Emphasis is placed on the translational relevance of these findings and the challenges that must be considered for successful clinical application. Table 4 shows the phenotypes rescued for each of the therapeutic approaches discussed in this section.

In the first published study (Daily et al. 2011) using AAV to replace *UBE3A*, the adult (P60) $Ube3a^{m-/p+}$ AS mice (model: Jiang 1998) received a single dose of rAAV vector (AAV9) containing a type two terminal repeat human *UBE3A* isoform 1 transgene, and the effects of *UBE3A* replacement were compared to WT animals, and AS mice given injections of AAV containing *GFP* without *UBE3A*, under identical conditions. Doses of 3 x 10^9 vg/mouse were delivered via bilateral parenchymal injections directly into the

Paradigm	Gene Re-instatement Model					AAV-GT				HSC-GT			ASO				CRISPR							ATF
Study	Silva-Santos (2015)					Daily (2011)	Nenninger (2022)	Judson (2021)	Born (2025)	Adhikari (2021)		Luthers (2025)	Meng (2015)	Milazzo (2021)		Lee (2023)	Schmid (2021)		Wolter (2020)	Li (2021)	Lu (STEP-RNP) (2025)			O'Geen (2023)
Treatment Age	Pre-natal	Birth	Juvenile	Adolescent	Adult	Adult	Adult	Birth	Birth	Birth	Adult	Adult	Adult	Birth	Juvenile	Adult	Birth	Juvenile	Birth	Birth	Birth	Juvenile	Adult	Adult
Synaptic Plasticity	n/a	n/a	G	G	G	L	L		n/a	n/a	n/a		G			n/a	L	G	G	L	L	L	n/a	G
Learning and Memory	n/a	n/a	n/a	n/a	n/a	G	L		n/a		n/a			n/a	n/a	n/a	L	L	R		n/a	G		n/a
Nest Building	G	R	R	R	L	n/a	n/a		n/a	n/a	n/a	n/a		R			G	G		n/a	n/a			n/a
Balance	n/a	n/a	n/a	n/a	n/a	n/a			n/a				n/a					n/a		n/a				n/a
Motor Coordination	G	G	G	R	R	G	G						R		G	G	L	L						n/a
Activity	G	R	R	R	G	n/a	n/a	R					G	G	L	L	L	L	R					n/a
Marble Burying	G	R	R	R	G	n/a	n/a		n/a	G	G	G	R	G	G		R		n/a		n/a	n/a	n/a	n/a
Hindlimb Clasp	n/a	n/a	n/a	n/a	n/a	n/a	G	G		n/a	n/a			G			G		G					n/a
Seizure Propensity	G	n/a	R	R	R	n/a	G	G		L		L	G	G	G	G	G		G		G	G		n/a
EEG	n/a	n/a	n/a	n/a	n/a	n/a	G			L	L	L	n/a	G	G		G		G		G			n/a
Weight	n/a	n/a	R	R	R	n/a	n/a	R	L	n/a	n/a	n/a	G	n/a	n/a	G	L	L	G		G			n/a

Table 4. Cross-modal summary of phenotype rescue across *UBE3A*-reactivation or replacement strategies and treatment ages in Angelman syndrome mouse models.
Heat map aggregating outcomes from studies that re-instate UBE3A by distinct modalities: conditional endogenous gene re-instatement (Gene Re-instatement Model), AAV-based gene therapy (AAV-GT), hematopoietic stem-cell–mediated delivery (HSC-GT), antisense oligonucleotides targeting *Ube3a-ATS* (ASO), CRISPR-based approaches (Cas9), and artificial transcription factors (ATF). Columns list representative referenced studies; rows list behavioral, electrophysiological, and anatomical readouts. "Treatment age" indicates the developmental age range at intervention (prenatal, birth, juvenile, adolescent, adult; described in Table 1). Color code: Green denotes full rescue: treated AS mice differ significantly from untreated AS controls and are statistically indistinguishable from wild type (WT) or meet an a priori criterion for full normalization. Light green denotes partial rescue defined by any of the following: approximately ≥80% of WT performance or level; significant improvement versus untreated AS controls while remaining significantly different from WT; not significantly different from WT or untreated AS, falling between the two values; or a sex-limited effect where only males or only females reach significance. Red denotes no rescue: the assay was performed, but no significant improvement over AS controls and a significant difference from WT was detected. White cells labeled n/a indicate that the assay was not performed or that AS and WT did not differ at baseline, precluding assessment of rescue. Paradigm definitions: **Learning and memory** encompass associative, spatial, or working memory assays. **Motor coordination** reflects rotarod performance; protocol differences across studies (for example, acceleration profiles and training schedules) may influence sensitivity. **Balance** reflects beam or dowel walking metrics. Protocol variations between laboratories may affect comparability. **Activity** reflects open-field locomotion. **Synaptic plasticity** primarily reflects hippocampal long-term potentiation. **Hindlimb clasp** reflects tail-suspension hindlimb splay. **Seizure** propensity reflects audiogenic seizure susceptibility. **EEG** reflects spectral abnormalities or epileptiform activity. **Weight** reflects body mass/obesity phenotypes.

hippocampus. Immunohistochemical quantification revealed that E6-AP protein expression reached approximately 100% of WT levels in the targeted hippocampal region with no evidence of overexpression in those regions. No expression was seen in the cortical region due to direct parenchymal hippocampal injection, which may explain the lack of improvement in tests of motor function, including rotarod, open field, and elevated plus maze test, in which *UBE3A*-treated animals showed no difference from *GFP*-treated animals (Daily et al. 2011). Hippocampal LTP, a hallmark synaptic deficit in AS mice, was measured in the WT, *UBE3A*- and *GFP*-treated mice. AS mice treated with *GFP* showed the expected LTP deficits: however, the post-tetanic potentiation and early phase of LTP of the *UBE3A* treated AS mice was equivalent to WT indicating partial restoration of synaptic plasticity in adult mice.

There was no significant difference between any of the groups during late-phase LTP (Daily et al. 2011). While motor deficits were not rescued, contextual fear memory was fully restored to wild-type levels, and spatial learning in the Morris water maze showed marked improvement with reduced latencies and increased platform crossings at 72 hours post-training, although quadrant-specific spatial bias remained inconsistent. While these early experiments were significant for demonstrating the potential of AAV-mediated *UBE3A* gene replacement, the clinical translatability of the study was limited for several reasons. The biodistribution of the treatment was limited to the hippocampus, limiting the conclusions that can be drawn about the degree of rescue achieved, as the route of administration used in these experiments would not be the route of administration for humans. Therefore, care should be taken when

attempting to utilize data from these early experiments to predict the efficacy of human AAV-mediated gene replacement therapies.

In a full *Ube3a* gene deletion rat model of AS, Nenninger et al. evaluated the efficacy of a novel secreted *UBE3A* construct (STUB) based on human isoform 1, delivered via bilateral intracerebroventricular (ICV) injection to young adult rats (age 3 months) (Nenninger et al. 2022). Six weeks post-injection, LTP in STUB-treated rats was fully restored to WT magnitude, while conventional *UBE3A* yielded only partial rescue in rats of the same age. Motor performance was significantly improved on the rotarod and hindlimb clasping assays with STUB, and both vectors normalized fear conditioning responses, though STUB showed superior efficacy. Importantly, STUB enabled intercellular UBE3A protein transfer through extracellular secretion and cross-correction, improving therapeutic effect in neighboring neurons, and addressing the limited biodistribution associated with conventional AAV delivery to the brain (Nenninger et al. 2022). In a separate set of experiments, young adult $Ube3^{m-/p+}$ AS mice (model: Jiang 1998) were dosed with 2×10^{10} vg/mouse via hippocampal injection, and the effects of UBE3A replacement on hippocampal electrophysiology were observed. AS mice treated with the vector containing the STUB construct demonstrated a complete recovery of the hippocampal LTP deficit (Nenninger et al. 2022).

Judson et al. used the $Ube3a^{m-/p+}$ AS mice (model: Jiang 1998) at age P0.5-P2 with an AAV vector containing a codon-optimized dual-isoform (iso1/iso2) of the human *UBE3A* transgene containing a Kozak sequence, under the control of the human synapsin promotor (hSYN), to enable physiological expression of both short and long isoforms at a ~3:1 ration (Judson et al. 2021). A single total dose of 1.6×10^{11} vg/mouse was delivered via bilateral ICV injection. At approximately six months post-treatment, UBE3A expression in different regions of the brain was assayed using immunofluorescence.

In AAV-treated AS mice, UBE3A protein expression reached 50–80% of wild-type levels, with the highest expression levels seen in the hippocampus and cortex and the lowest observed in the cerebellum (Judson et al. 2021). Functional phenotypic rescue was observed

in seizure susceptibility assayed by flurothyl-induced seizure, motor learning including rotarod and open field test, and innate behavioral assays including marble burying and nest building (Judson et al. 2021). By two months post-treatment, both vehicle-treated and AAV-treated female AS mice exhibited excessive weight gain relative to WT female mice. While the body weight changes for male AS mice were not statistically significant, the excessive weight gain in the female AS mice, regardless of treatment with AAV, suggests that the AAV treatment was unable to normalize the weight-gain phenotype (Judson et al. 2021).

Critically, WT mice treated with the AAV-h*UBE3A* vector exhibited UBE3A overexpression in the neocortex of approximately 150%, however, this regional overexpression did not negatively affect phenotype, supporting tolerability of this dual-isoform construct at the doses tested (Judson et al. 2021).

Born et al. at the University of Pennsylvania (now GEMMA Bio) reported that unilateral ICV delivery at P0/1 using the AAV-hu68 capsid carrying the human *UBE3A* isoform 1 transgene, resulted in improvements in key behavioral and motor phenotypes. Using the $Ube3a^{m-/p+}$ mouse model (model: Jiang 1998), ICV delivery at doses 4 doses ranging from 2.5×10^{10} GC/mouse (low dose) to 1.85×10^{11} GC/mouse (high dose) resulting in a dose-dependent correction of phenotype in the AS model including improvement in body weight, rotarod performance, hind limb clasping, and nest building. These improvements correlated with a similar dose-dependent increase in *UBE3A* transcript and protein expression throughout the brain, reaching 60-90% of WT levels in neurons (Born et al. 2025).

Collectively, these studies provide converging evidence that AAV-mediated gene replacement therapy can restore therapeutically relevant levels of UBE3A and result in meaningful phenotypic rescue, even when administered at varying postnatal timepoints with a single isoform. While early postnatal delivery yielded robust outcomes in the AS mouse model, it is challenging to compare the studies to each other, as the studies were not performed using comparable ROAs, vectors, or doses. However, all studies demonstrated neuronal transduction, stable expression, and marked improvements in phenotype

(Table 4). These data suggest that phenotypic recovery is not exclusively restricted to early therapeutic windows. Gene delivery at later postnatal stages may provide significant rescue of molecular and behavioral deficits, indicating that the therapeutic window for intervention could be broad. This temporal flexibility, coupled with advances in vector design such as optimized capsids, neuron-specific promoters, more translatable routes of administration, dose optimization, and varying isoform constructs support the potential for AAV-based therapies to benefit a wide patient population, including those diagnosed beyond infancy and those of all genotypes (Table 4).

Despite this progress, key translational challenges remain, including isoform specificity, immunogenicity, pan-neuronal biodistribution, and long-term safety validation. Of these, the question of the translatability of AAV biodistribution is a particular challenge, as multiple studies have shown differential patterns of biodistribution in mice vs. nonhuman primates, even when using capsids considered to be neurotropic (Gray et al. 2011; Liguore et al. 2019; Chauhan et al. 2024; Drouyer et al. 2024). The differences in AAV biodistribution make dose prediction and generation of PK/PD relationships more difficult. However, these difficulties will be resolved as more AAV-directed gene therapies targeting neurons are tested in humans, and this challenge should not diminish the expanding body of evidence underscoring the transformative promise of AAV gene therapy as a durable, mechanism-targeted intervention for individuals with AS.

Hematopoietic Stem Cell Lentiviral Vector-Mediated Ex-Vivo Gene Replacement Therapy (HSC-GT)

Another potential therapeutic strategy for the treatment of AS and other neurogenetic disorders, is ex-vivo autologous hematopoietic stem cell gene replacement therapy (HSC-GT). These HSCs can be modified using a lentiviral vector to deliver a healthy copy of the *disease transgene* to early blood stem cells for gene delivery to the entire body. Neurologic disorders such as Metachromatic Leukodystrophy (MLD), Cerebroadrenoleukodystrophy (CALD), and Fanconi Anemia have shown promising human clinical data of complete neurologic correction after HSC-GT (Riedel et al. 2024; Lauer et al. 2023; Rockwell et al. 2025). In AS, the same technique has been used to introduce modified hematopoietic stem cells (CD34+) to the bone marrow, where they engraft. The white blood cell lineage is then able to circulate peripherally and cross the blood brain barrier with immune cells engrafting in the CNS as presumed microglia, secreting a modified version of the UBE3A protein to neighboring neurons resulting in cross correction and diffuse pan-neuronal biodistribution (Luthers et al. 2025; Adhikari et al. 2021). Adhikari et al. transduced human CD34+ cells with a lentiviral vector carrying a modified secretory version of mouse *Ube3a* (LVV-*Ube3a)* and subsequently transplanted the transduced cells into an immunodeficient strain (*IL2* deficient) of $Ube3a^{m-/p+}$ mice at P2-5 or P28-35 (Adhikari et al. 2021). Eight weeks post-transplant AS mice treated at P2-5 or P28-35 with LVV-*Ube3a* transduced cells exhibited improved performance on open field locomotion, balance beam and rotarod (Adhikari et al. 2021). These constructs contained the MNDU3 promoter, which has since been implicated in the development of insertional oncogenesis in CALD (Duncan et al. 2024), with the development of myelodysplastic syndrome in approximately 10% of patients with CALD. Due to these developments, additional work with safer promoters was undertaken (EFS and hPGK), with EFS having a safety track record of over 500 patient years of data (Booth et al. 2025). These studies using alternative promoters were conducted in the more traditional AS mouse model (model: Jiang 1998) at an adolescent/adult age, using mouse CD34+ cells transduced with the *mUbe3a* transgene. These studies, testing both alternative promoters, replicated the findings of Adhikari et al. achieving complete rescue of all behaviors in an adult AS mouse, including complete correction of the increased EEG spectral power. (Luthers et al. 2025). Due to the ability of CNS immune cells to engraft throughout the brain, biodistribution to deep brain structures was possible, which could explain the exceptional neurobehavioral rescue results. Overall, similar results were obtained using 3 different promoters (MNDU3, EFS, hPGK) at both young and advanced ages in 2 different laboratories, supporting strong evidence of potential benefit in an extended age range. The diffuse brain biodistribution with this approach is likely the reason why such profound phenotypic rescue was observed (Table 4).

CRISPR Unsilencing of the Paternal Allele:

CRISPR (clustered regularly interspaced short palindromic repeats) technology is a potentially powerful tool for treating genetic diseases, and the first CRISPR-based therapeutic, exagamglogene autotemcel, was approved to treat Sickle Cell Disease in the United States in 2023 (Frangoul et al. 2021). In the context of AS the most obvious application of CRISPR-Cas9 technology is permanent unsilencing of the paternal allele by targeting the *UBE3A-ATS*, disrupting its transcriptional elongation through DNA editing of targeted repeats through sequence dependent sgRNAs. This may alleviate transcriptional interference and allows reactivation of the paternal *UBE3A* allele. Alternatively, catalytically inactive Cas9 (dCas9) fused to transcriptional repressors such as KRAB can be targeted to the *UBE3A-ATS* promoter to silence its expression epigenetically without inducing DNA breaks. Both approaches rely on guide RNA-directed targeting of the *UBE3A-ATS* and aim to restore *UBE3A* expression selectively in neurons, making it highly suitable for addressing the unique molecular pathophysiology of AS.

While CRISPR as a potential treatment for AS has yet to be tested in humans, there have been several mouse studies conducted by multiple groups that use CRISPR to truncate the *Ube3a-ATS* transcript, resulting in a reactivation of the paternal *Ube3a* gene. Wolter et al., demonstrated the long-lasting therapeutic potential of a CRISPR-based gene editing approach by targeting the paternal *Ube3a* allele using an AAV vector (Wolter et al. 2020). In these experiments, a dual-injection strategy was developed using a neuron-specific AAV9 vector encoding *Staphylococcus aureus* Cas9 (SaCas9) and a highly multiplexed guide RNA (Sajw33) targeting the *Snord115* gene cluster representing a neuronally expressed region of the *Ube3a-ATS* transcript. Repeat ICV injections of the vector in the $Ube3a^{m-/p+}$ AS mouse model (model: Jiang 1998) at embryonic day 15.5 and P1 (1.5×10^{10} vg/ventricle) yielded widespread, persistent expression of paternal *Ube3a* across cortical layers, the hippocampus, and the spinal cord in mice, achieving ~40% of wild-type protein levels (Wolter et al. 2020). Treated animals showed partial reversal of microcephaly with a statistically significant increase in brain weight relative to untreated AS mice. Treated mice also exhibited statistically significant

improvements relative to untreated AS mice in motor and behavioral tasks, including hindlimb clasping, open-field center time, and rotarod performance that persisted beyond seven months of age. However, improvements were limited in measures of anxiety-like behavior (e.g., marble burying) and locomotor activity as measured by open field distance traveled (Table 4) (Wolter et al. 2020).

In a separate experiment, the vector was delivered via single ICV injection at embryonic day 15.5, and the animals were followed for 17 months. In those animals, paternal Ube3a expression was appropriately localized to the nucleus and persisted for at least 17 months, with no off-target genomic editing documented, no evidence of neuroinflammation, and no disruption to the *Snord115* target gene expression or splicing (Wolter et al. 2020).

A similar set of experiments were performed by Schmid et. al, in which $Ube3a^{m-/p+}$ (model: Jiang 1998) mice were injected at P0-1 ICV bilaterally with an AAVhu68 vector carrying Cas9 and a sgRNA targeting *Ube3a-ATS* at a dose of 1×10^{11} GC/mouse (Schmid et al. 2021). Analysis of the gene editing efficiency post-injection indicated approximately 20% of neurons were edited, and treated animals had Ube3a expression of 25-40% of wild type levels (Schmid et al. 2021). At eight weeks post-injection, treated and non-treated mice were assayed for phenotypic changes for three consecutive days, including rotarod, nest building, marble burying, open field ambulatory activity and body weight (Schmid et al. 2021). At days two and three, treated mice showed a statistically significant improvement in rotarod performance when compared with untreated $Ube3a^{m-/p+}$ mice, although the treated animals rotarod performance did not match that of WT animals. Treated animals showed statistically significant improvements in marble burying and nest building activities when compared to untreated animals, and again treated animals did not match the performance of WT animals in either test (Schmid et al. 2021). Open field ambulatory activity was not significantly different between treated and untreated groups. Animals injected at P14, P21, and P28 showed significantly less editing (>5%) and were not subject to subsequent phenotypic assays.

A novel RNP-based CRISPR gene-editing platform delivered via surface tailored assembly (STA) called

STEP-RNP (Stimuli-responsive traceless engineering platform-ribonucleoprotein) (Jiang et al 2024; Lu et al 2025) has been recently developed as a therapeutic strategy for AS. A STEP-RNP complex containing a guide RNA targeting the *Ube3a-ATS* was delivered via intrathecal injection to $Ube3a^{m-/p+}$ mice (model: Jiang 1998) at three distinct ages: neonatal (P1), juvenile (P21), and adolescent (P42) (Jiang 2024; Lu et al. 2025). In all age groups, molecular assessment of brain tissue confirmed efficient gene targeting and disruption of the *Ube3a-ATS*, leading to robust reactivation of paternal *Ube3a* expression in cortical and hippocampal neurons. Treatment with the complex at any age restored Ube3a protein levels to approximately 60–80 % of wildtype levels, which was sustained for at least 8 months post-treatment. Animals treated at any age demonstrated improvements on the open field test, with performance approaching that of wild type animals. Similar effects were seen on the Rotarod, treated animals from any age group had improved performance in both the accelerated and steady paradigms (Lu et al. 2025). Long- and short-term memory as assessed by novel object recognition showed that short term memory was improved only in animals treated at P1, while long term memory was improved in animals treated at any age. Treatment with the *Ube3a-ATS* STEP-RNP complex also corrected both myoclonic and tonic seizures in animals treated at any age (Jiang 2024; Lu et al. 2025) (Table 4).

The effect of treatment with the *Ube3a-ATS* STEP-RNP complex is also being evaluated in an ongoing study in the $LD^{m-/p+}$ AS mouse model. Animals were treated with a single dose of the *Ube3a-ATS* STEP-RNP complex at P21, and their performance on a battery of behavioral and cognitive tests was compared to untreated $LD^{m-/p+}$ AS mice. Similar to effects seen with the $Ube3a^{m-/p+}$ mice, treatment with the *Ube3a-ATS* STEP-RNP complex resulted in improvements in performance on the open field test, with treated animals' performance restored to near-WT (Jiang 2024). The treated LD mice also showed improvements on the Rotarod; in the accelerating paradigm the treated mice performed slightly better than untreated animals, however, in the steady state paradigm, the treated animals performed nearly as well as WT littermates. These data are significant, not only because they demonstrate the STEP-RNP

platform's capacity to achieve longterm, brainwide paternal *Ube3a* unsilencing and subsequent phenotypic rescue, but also because they demonstrate that phenotypic rescue is possible at a broad range of ages, and further, that it is possible with the large chromosomal deletion (~6MB) that represents the majority of AS individuals.

Artificial Transcription Factors/Zinc Finger for Paternal *Ube3a* Activation

Another approach to paternal unsilencing involves engineering a zinc finger protein (ZFP) to target the *UBE3A-ATS*. Zinc finger proteins are ubiquitous cellular transcription factors, which can carry a Kruppel-associated box (KRAB) domain, that facilitates gene-specific repression. Bailus et al described the screening and development of an ATF targeting the *Ube3a-ATS*, linked to a cell-penetrating peptide to facilitate blood brain barrier crossing, which was designated as TAT-S1 (Bailus et al. 2016). TAT-S1 was administered subcutaneously to $Ube3a^{m-/p+}$ AS mice (model: Jiang 1998), at doses of 160-200 mg/kg three times per week for a total of four weeks. Following the treatment regimen, *Ube3a* was significantly increased in the brains of the treated AS mice, relative to untreated animals. In addition, broad distribution of the ATF was observed throughout the brains of treated animals (Bailus et al. 2016). These experiments demonstrated the feasibility of an ATF to unsilenced paternal *Ube3a* expression; however, several technical limitations were identified which necessitated a change in the route of administration. In a follow up study, O'Geen et al described the delivery of the ATF (AAV-SK1) previously described by Bailus et. al, (Bailus et al. 2016; O'Geen et al. 2023), using an AAV vector that can cross the blood brain barrier in mice following IV injection, AAV-PHB.eB (Mathiesen et al. 2020). Six-week-old AS mice (model: Jiang 1998) were administered AAV-SK1 at 1×10^{12} vg/animal via tail vein injection. Five weeks post-injection, Ube3a protein in treated animals had been increased to 26% of WT levels, and the average number of Ube3a positive cells in the brains of treated mice were comparable to those observed in WT; 76% in the prefrontal cortex, 83% in the hippocampus, 80% in the cerebellum, and 45% in the striatum (O'Geen et al. 2023). *Ube3a-ATS* transcript was decreased by 2.2-fold in AAV-SK1 treated-animals relative to untreated

animals. The treatment was well-tolerated, and there was no detection of off-target impact on global gene expression, and no upregulation of immune-specific genes suggestive of an immune response (O'Geen et al. 2023).

Changes in motor phenotypes were assessed following treatment with AAV-SK1 using the open field, Rotarod, and DigiGait analysis. AS mice treated with AAV-SK1 demonstrated improved performance in the open field test, with total activity values restored to WT levels, and DigiGate analysis showed restoration of stride frequency to WT levels, yet there was no significant improvement on the Rotarod when compared to untreated animals (O'Geen et al. 2023). These data indicate that treatment with ATFs can restore Ube3a to approximately 27% of WT levels, and this is sufficient for adolescent/adult mice to achieve improvement in various phenotypes (Table 4).

Antisense Oligonucleotide (ASO) Treatments for *UBE3A* Reactivation

An ASO targeting the *UBE3A-ATS* transcript functions by selectively degrading the long non-coding RNA which normally silences the paternal *UBE3A* allele in neurons. By disrupting the *UBE3A-ATS*, an ASO enables reactivation of the otherwise epigenetically repressed paternal allele.

The first proof-of-concept studies on the utility of an ASO for AS were reported by Meng et al. using an ASO sequence targeting the mouse *Ube3a-ATS* (Meng et al. 2015). Meng, et al. coupled this approach with the use of the paternal *Ube3a* YFP reporter mouse model, which enabled direct visualization and quantification of paternal Ube3a protein expression from inserting a yellow fluorescent protein (YFP) tag into the endogenous silenced paternal *Ube3a* locus of otherwise wild-type mice (Meng et al. 2015). This treatment reduced the *Ube3a-ATS* RNA levels by 60–70%, leading to a 2–5-fold increase in paternal *Ube3a-YFP* transcript and partial restoration of Ube3a-YFP protein to 82% in the cortex, 33% in the hippocampus, and 73% in the spinal cord relative to maternally expressing controls after ICV delivery. Protein reactivation was stable for up to 16 weeks and spatially widespread, with no adverse effects on glial activation or nearby imprinted genes such as Snord116 (Meng et al. 2015). Behavioral rescue in treated adolescent/adult (P30-60) *Ube3a*$^{m-/p+}$ *AS* mice (model:

Jiang 1998) included normalization of contextual fear conditioning and a sustained correction of the obesity phenotype, although no improvements were observed in marble burying, open field, or rotarod performance (Meng et al. 2015).

Milazzo, et al. (Milazzo et al. 2021) developed a novel ASO targeting *Ube3a-ATS*, RTR26266, based on in vitro knockdown and upregulation of *Ube3a* expression, as well as favorable in vivo tolerability (Milazzo et al. 2021). A single dose of RTR26266 was delivered by ICV injection at P1 in the *Ube3a*$^{m-/p+}$ AS mice (model: Jiang 1998). Ube3a was detected in treated AS mice one-week post-injection, and at two weeks widespread brain-wide Ube3a protein reinstatement was observed, with a peak expression of approximately 70-80% relative to WT. The percent of Ube3a observed in the treated AS mouse brains declined from the two-week maximum to approximately 20% of WT levels by 9 weeks post-injection (Milazzo et al. 2021) (Table 4).

Similar to Meng et al., behavioral rescue was domain-specific but revealed a greater positive effect on the established AS mouse model phenotype, showing that P1-treated AS mice exhibited normalized behavior on the open field test and improved performance in the forced swim test and reverse rotarod. However, repetitive and innate behaviors such as marble burying and nest building remained impaired (Milazzo et al. 2021). Seizure susceptibility was completely abolished, and hippocampal synaptic plasticity, as measured by long-term potentiation (LTP), was restored to wild-type levels. Anatomically, there was a trend toward correction of microcephaly, though not statistically significant (Milazzo et al. 2021). To test the efficacy of later intervention, juvenile (P21) AS mice received a single ICV dose of RTR26266. This treatment also resulted in broad reactivation of *Ube3a* across multiple brain regions and cell types, with protein levels reaching 50–99% of wild-type depending on the region. Audiogenic seizure susceptibility was fully rescued, supporting the existence of a broader therapeutic window for seizure phenotypes. However, hippocampal LTP was only modestly improved and did not reach statistical significance. Other behavioral and cognitive assessments were not assessed in this study (Milazzo et al. 2021).

Finally, a comparative study from Lee, et al., evaluated novel ASOs targeting *Ube3a* and *Snord115* antisense transcripts for paternal *Ube3a* expression in the *Ube3a^{mΔe6/p+}* AS mouse model, which was created to ensure full knockout of *Ube3a* in the brain (model: Lee et al. 2023). When administered to juvenile mice (P21–24), both ASOs produced a statistically significant increase in *Ube3a* mRNA and protein levels relative to animals treated with a non-targeting control ASOs. Both ASO's suppressed *Ube3a-ATS* across multiple brain regions and the effect was observed to last approximately 10 weeks. When adult (P56-72) *Ube3a^{mΔe6/p}* mice were treated with either the *Ube3a* or *Snord115* ASO, a statistically significant increase in Ube3a protein was observed in the anterior cortex and hippocampus, suggesting that there is potential for some rescue in adult animals (Lee et al. 2023). Using EEG as a functional readout of treatment effects, treatment of juvenile animals with the ASOs resulted in the observation of a decrease of the power in the alpha, low beta, and high beta bands and an increase of the power in the high gamma band, resulting in a normalization of the $(α + β1 + β2)/γ2$ ratio in the frontal and somatosensory cortices particularly at 3 and 6 weeks post ASO injection. Treating the adult *Ube3a^{mΔe6/p}* mice also resulted in improvements in EEG, the power in the low frequency bands was reduced and the power in the high gamma band was increased in the frontal cortex thereby reducing the $(α + β1 + β2)/γ2$ ratio to near that of WT animals (Lee et al. 2023). Juvenile and adult ASO treated animals had improvements in sleep, showing normalization of REM and non-REM sleep to WT levels that was maintained for up to 10 weeks post-injection (Lee et al. 2023). At both treatment ages, the improvements occurred in a Ube3a protein dependent manner, as the effects waned as Ube3a protein levels decreased (Lee et al. 2023). While improvements were seen in sleep and EEG rhythms in treated animals relative to control animals, neither ASO substantially reduced the frequency of poly-spikes observed by EEG in juvenile or adult treated animals. EEG traces from the left frontal cortices, left somatosensory cortices and right visual cortices show increased poly-spike activity in ASO treated animals relative to control or WT animals. These data indicate that under the experimental conditions used in the study, the degree of Ube3a restoration was not sufficient to fully resolve the cortical hyperexcitability (Lee et al. 2023),

suggesting either higher Ube3a expression is needed to show significant phenotypic rescue and that increased Ube3a expression would show a greater effect for established seizure control. Interestingly, in this study, the pathognomonic delta power phenotype in this mouse model/strain was not robust enough at baseline compared to WT or after ASO treatment to confirm a change that has been seen with the original Jiang et al 1998 mouse model (Table 4).

The totality of the data in the AS mouse models suggests that ASOs are a viable option for treatment of AS, however, when comparing experiments performed in different laboratories, it is important to remember that dose is not the only parameter that may impact outcome. The specific sequences of the individual ASOs, chemical modifications, relative purity, and delivery medium may all play a role in the biodistribution, durability of effect, and ultimately efficacy.

The contrast in behavioral recovery observed under different conditions (Table 4) as seen in the Cre-lox system compared to that observed when the AS mice are treated with all number of therapeutic modalities aimed at restoring Ube3a, suggest that potentially confounding variables inherent to the Cre-lox system may limit the amount of behavioral recovery that is possible in this model for certain neurodevelopmental disorders. This contrast is further supported by ongoing Phase 1/2 clinical trials of ASOs. Preliminary data from open-label trials report behavioral improvements across a wide range of patient ages (4-17 years of age for Ultragenyx, 2-50 for Ionis, and 1-12 for Roche) (NCT04259281, NCT05127226, NCT04428281) Subgroup analysis based on various ages of development have not yet been available for the human clinical trials, but significant improvements have been reported by all sponsors across all ages indicates that a wide range of patients will benefit from therapeutic interventions. The observed improvements in AS patients treated with ASOs, albeit open-label, are equally reported in broad age ranges by all sponsors, demonstrating the potential for therapeutic benefit may not be limited to the youngest patients, and that human clinical data will be more reflective of the possible human benefit than any experiment can be in a mouse model.

Current Human Proof of Concept Clinical Data for Novel AS Therapeutics

Beginning in 2020, clinical trials using intrathecally delivered antisense oligonucleotides (ASOs) were initiated, and since that time there have been three ongoing open-label Phase 1/2 clinical trials using three distinct ASOs, all of which target different regions of the *UBE3A-ATS* in individuals living with AS. Participants ranged in age from 1 to 50 years (NCT04259281, NCT07157254, NCT04428281, NCT05127226) and include individuals with large deletions and intragenic mutations. A recent publication summarizes the Phase 2 data from one of these trials (Hoffman-LaRoche; Hipp et al. 2025) This study describes the safety, tolerability, and pharmacokinetics of rugonersen (RO7248824) and included children ranging in age from 1-12 (inclusive) with a confirmed diagnosis of AS including the deletion or mutation genotypes. The study included within-participant dose-escalation to explore multiple dose levels, various dosing regimens of time interval of dosing, and was followed by a long-term extension phase to collect additional safety and tolerability data. Fifty participants were enrolled in this multiple ascending dose (MAD) portion of the study, and all received two or three intrathecally delivered doses of rugonersen ranging from 6 mg to 180 mg in the first two months. Doses were escalated across all cohorts, with the older cohort (ages 5-12) escalating before the younger cohort (ages 1-4), with the total dosing plus the post-treatment period being >= 225 days (Hipp et al. 2025). Of the initial 50 enrolled participants, 49 continued to the long-term extension in which some participants received 120 mg every 12 weeks, and others 180 mg every 24 weeks. In addition, an additional cohort of 11 participants received a 60 mg dose every 16 weeks. Overall, rugonersen was reported to be relatively well tolerated with no participants withdrawing from the study due to adverse events. Twenty-one participants (34%) experienced at least one serious adverse event (SAE), and the SAEs of 8 participants (13%) were classified as drug related. The total number of AEs were 1225, of which 503 were classified as drug related (Hipp et al. 2025).

EEG was measured as a pharmacodynamic marker of rugonersen activity. The change in EEG delta power was recorded and compared both to the participants own pre-treatment baseline values, and an age matched AS natural history study (NHS) reference value. On day 55 post-dosing, following two doses of rugonersen, the EEG delta power decreased -27.9% below the AS NHS reference, and by day 100, the EEG delta power decreased -41.3% below the AS NHS reference (Hipp et al. 2025). At 100 days, approximately 14 weeks post-last dose of rugonersen, and at day 224 (24 weeks post-last dose), the EEG delta power started to increase back to the AS NHS reference range. A more detailed analysis of the EEG delta power at day 100 post dosing indicated that the decrease was dose-dependent and was more pronounced for older participants. In the long-term extension, the quantitative EEG delta power decrease was the most persistent in the cohorts receiving 120 mg of rugonersen every 16 weeks when compared to the AS NHS reference, whereas the groups receiving 180 mg every 24 weeks or 60 mg every 16 weeks did not display a difference relative to the AS NHS reference, presumably because these were trough assessments and the ASO was no longer active at the time the time of the assessment (Hipp et al. 2025).

On the Bayley Scale of Infant Development-third edition (BSID-III) and the Vineland Adaptive Behavior Scales-third edition (VABS-3), participants in the MAD cohorts showed greater increases in growth score values than the AS NHS reference values over the same time frame, in all five VABS domains (including personal daily living skills, receptive communication, expressive communication, fine motor, and gross motor) , and four of the five BSID domains (cognition, receptive communication, expressive communication and fine motor, but not gross motor). The observed differences in rate of gain between the ASO-treated and NHS groups were comparable to the magnitude estimated to be minimally clinically important (Hipp et. al 2025) based on work that was done through the support of the Angelman Syndrome Biomarker and Outcome Measure Consortium (A-BOM). Similarly, on the Symptoms of Angelman Syndrome-Clinician Global Impression (SAS-CGI) assessment of symptom change (SAS-CGI-Change), the apparent change in symptoms above the AS NHS baseline was consistent, with approximately 74% of participants having an improvement in the SAS-CGI-Change. Changes in the BSID, VABS, and SAS-CGI-Change were also

observed in the long-term extension and were of generally greater magnitude than the estimates of minimal clinical importance for the BSID, based on the assessment determined by an MCID study (Hipp et al 2025). All dose regimens in this study showed similar magnitude of difference from the NH reference on BSID and VABS assessments, however, direct comparison of the dose groups is complicated by the differences in the timing of the doses and assessments as well as the variability in the dosing and testing regimen for each cohort (Hipp et al 2025).

The positive changes observed in AS individuals treated with rugonersen are encouraging, however interpretation of open-label data is more complex than data from a blinded placebo- or sham-controlled trial, since expectation bias and other confounding variables; variable dosing regimens, genotypes, ages, and dose intervals or pauses need to be carefully considered in data interpretation. Hoffman-LaRoche discontinued development of rugonersen in 2023, stating that the observed level of clinical efficacy was insufficient to meet Roche's internal standards (Roche press release, July 6 2023), however, in 2025, the rights to develop rugonersen was acquired by Oak Hill Bio, and a phase 3 pivotal trial is expected to begin in 2026 (OHB press release April 15, 2025).

A second ASO, apazanersen (GTX-102; Ultragenyx Pharmaceuticals) completed their Phase 1/2 open label clinical study (NCT04259281) and has since completed enrollment of their Phase 3 sham-controlled clinical trial in July 2025 (ASPIRE, NCT06617439). The open-label, Phase 1/2, multiple ascending dose (MAD) study of GTX-102 enrolled 74 children with large deletions, ages 4-17, inclusive. Participants were administered 3 or 4 monthly loading doses followed by quarterly maintenance dosing, and the safety, tolerability, and pharmacokinetics of apazanersen were assessed. Performance on outcome measures were compared to an age and genotype matched longitudinal cohort from the AS natural history study. Apazanersen was considered generally well tolerated, with approximately 15% of patients experiencing a treatment-related adverse event, and no participants withdrew from the study due to adverse events (Goodspeed 2024).

Cognition assessed by the Bayley-4 (BSID-4) neurodevelopmental assessment showed rapid and statistically significant improvement in rate of developmental gain compared with age-matched prospective AS NHS data controls. Behavior assessed by the Angelman Severity Assessment (ASA) showed rapid improvements exceeding baseline in multiple domains determined meaningful by the disease concept model (challenging behaviors, sleep, communication, gross motor function), and hyperactivity and noncompliance, as assessed by the Aberrant Behavior Checklist-Community (ABC-C), showed significant improvement when compared to baseline and compared to the data collected in the longitudinal NHS. In addition, cognition and receptive communication assessed by BSID-4 showed clinically significant improvements compared to baseline and/or age-matched AS NHS data. The Multi-domain Responder Index (MDRI) analysis across the four domains of cognition, receptive communication, behavior and sleep resulted in a total net response of +2.0 (p-value <0.0001) (Tandon et al. 2021; Goodspeed 2024). Most patients achieved a total net response of +2 to +4 in multiple clinical domains, demonstrating improvement exceeding the minimally important difference (MID) threshold presented at the 2024 ABOM conference by Sadhwani et al. 2024 (Goodspeed 2024).

The third ASO in clinical trial is ION582 (Ionis Pharmaceuticals NCT05127226), who initiated their clinical development program in 2022 and is currently enrolling their Phase 3 placebo-controlled clinical trial (NCT06914690, REVEAL) after reporting positive Phase 1/2 clinical data (Ionis press release, July 22, 2024). The phase 1/2 study enrolled 51 participants ages 2 to 50, with either the large deletion or mutation genotypes, in an open label, MAD study. The end of phase 1/2 data by Ionis Pharmaceuticals (Ionis press release, July 22, 2024) reported that ION582 showed favorable safety and tolerability at all dose levels. Evidence of consistent benefit was observed across all ages and genotypes tested as well as clinical improvement in rate of gain was observed across the key functional areas including communication, cognition and motor function, exceeding the AS NHS rate of gain over the same time period on the BSID-4, the VABS-3, and communication abilities on the Observer-Reported Communication Ability

(ORCA). At 18 months of treatment, 97% of patients showed a meaningful response (defined as a change in baseline of >20% the standard deviation plus the expected change for growth from natural history study) in one or more domains of the Bayley-4, while 83% showed a meaningful response on 2 or more Bayley-4 domains, and 71% of patients showed a meaningful response to 3 or more Bayley-4 domains. 71% of patients showed a clinically meaningful response on the Bayley-4 expressive communication domain after 18 months of treatment (Ionis Innovation Day, October 7, 2025).

The human data and its implications for future therapeutic strategies:

Emerging data, albeit preliminary and from open label studies, from the ongoing ASO clinical trials targeting the paternal *UBE3A-ATS,* suggest that *UBE3A* reactivation may result in a meaningful clinical change in individuals living with AS. The human clinical trial data is in broad agreement with the majority of pre-clinical data obtained from multiple laboratories globally, all of whom used the genetically comparable AS mouse models, (Jiang et al, Lee et al). In these pre-clinical studies improvements in cognition, motor coordination and balance, learning and memory, sleep, EEG, and anxiety-like behaviors was achieved, regardless of treatment age. The data from the mouse models suggested that numerous approaches may lead to restoration of *Ube3a* expression and have the potential to lead to meaningful clinical benefit for individuals with AS, despite the obvious and significant differences between the brains of mice and humans. What was not anticipated by the AS mouse model(s) data is the impact on symptoms like expressive and receptive communication, activities of daily living, fine motor skills, and quality of life, which are not easily captured in rodent models. The results of the ongoing controlled studies will be critical to further define clinically meaningful improvements in this population, and ultimately how these data correlate to the pre-clinical experiments of different ages and different genotypes.

What is equally important to recognize is that the various therapeutic modalities tested in the AS mouse model(s) show a moderately different breadth of therapeutic benefit, with some more robust than others, regardless of age. This finding is likely related to a few factors: 1) a therapeutic that provides the most diffuse neuronal biodistribution (driven by dose, ROA, neuronal tropism, etc) and 2) a therapeutic that provides a long durability of effect for sustained Ube3a/UBE3A exposure, allowing the time necessary for learning. Taken together, the future of therapeutic interventions for humans living with Angelman syndrome is exciting, with the first clinical trial of an AAV-mediated gene replacement therapy expected to begin as a first-in-human Phase 1/2 trial in late 2025 (NCT07181837).

Building on this, Adrian Bird's landmark Rett syndrome study demonstrated that re-introducing functional MECP2 after symptom onset, particularly in adult mice, rapidly reversed major neurological deficits, normalized breathing and activity, and extended lifespan, thereby overturning the assumption that a narrow early "critical period" strictly limits therapeutic benefit (Guy et al., 2007). The key message of how this relates to Angelman syndrome is not that the disorders are identical, but that significant circuit plasticity can persist well beyond early development when the causal molecular obstacle is addressed. This specific precedent strengthens the findings in the AS mouse model of full phenotypic rescue seen with some modalities, regardless of age, and supports the rationale for testing AS therapies across a broad age range. In summary, while some therapeutic models for various conditions suggest the importance of early intervention by demonstrating the failure to rescue key behaviors at later stages, translational therapeutic interventions in the more traditionally used AS mouse model seem to contradict these findings.

This paradigm is not absolute, and as discussed here, has been challenged by multiple experiments and multiple laboratories using many different therapeutic mechanisms of *Ube3a* replacement or re-instatement, while nearly all have shown a positive impact on neurobehavioral phenotypes at each developmental stage. The possibility of therapeutic intervention has been clearly demonstrated in numerous experiments using the most human-relevant mouse model and multiple therapeutic interventions with direct translatability to humans. These advances represent significant potential for meaningful benefit to patients living with AS today, regardless of their age (Table 4). Indeed, earlier intervention may ultimately result

in the greatest clinical benefit, at a time where neuroplasticity is greatest and neurons have the greatest chance for manipulation and change, but an overwhelming majority of the available data strongly support the potential for meaningful benefit even in adults living with AS, suggesting that clinical trials should be inclusive of all ages from prenatal through adulthood. Once safety is established in postnatal humans for the different therapeutic strategies, the natural next step is to evaluate if improved results can be achieved in a developing fetus in utero prior to the development of any symptoms of Angelman syndrome. Work here is already underway (Clarke, 2024)

Future research analyzing phenotypic recovery across various therapeutic modalities, genotypes and ages will hopefully give a more robust and comprehensive understanding of each variable and help to determine what might provide the greatest benefit to each specific population. This understanding will help to maximize the true benefit of each therapy across diverse developmental contexts and help to drive decision making in one, or a combination, of therapeutic options.

References

Adhikari, A., N. A. Copping, J. Beegle, D. L. Cameron, P. Deng, H. O'Geen, D. J. Segal, K. D. Fink, J. L. Silverman, and J. S. Anderson. 2021. 'Functional rescue in an Angelman syndrome model following treatment with lentivector transduced hematopoietic stem cells', *Hum Mol Genet*, 30: 1067–83.

Albrecht, U., J. S. Sutcliffe, B. M. Cattanach, C. V. Beechey, D. Armstrong, G. Eichele, and A. L. Beaudet. 1997. 'Imprinted expression of the murine Angelman syndrome gene, Ube3a, in hippocampal and Purkinje neurons', *Nat Genet*, 17: 75–8.

Avagliano Trezza, R., M. Sonzogni, S. N. V. Bossuyt, F. I. Zampeta, A. M. Punt, M. van den Berg, D. C. Rotaru, L. M. C. Koene, S. T. Munshi, J. Stedehouder, J. M. Kros, M. Williams, H. Heussler, F. M. S. de Vrij, E. J. Mientjes, G. M. van Woerden, S. A. Kushner, B. Distel, and Y. Elgersma. 2019. 'Loss of nuclear UBE3A causes electrophysiological and behavioral deficits in mice and is associated with Angelman syndrome', *Nat Neurosci*, 22: 1235–47.

Bailus, B. J., B. Pyles, M. M. McAlister, H. O'Geen, S. H. Lockwood, A. N. Adams, J. T. Nguyen, A. Yu, R. F. Berman, and D. J. Segal. 2016. 'Protein Delivery of an Artificial Transcription Factor Restores Widespread Ube3a Expression in an Angelman Syndrome Mouse Brain', *Mol Ther*, 24: 548–55.

Baker, E. K., C. F. Merton, W. H. Tan, T. Dudding-Byth, D. E. Godler, and A. Sadhwani. 2022. 'Methylation analysis and developmental profile of two individuals with Angelman syndrome due to mosaic imprinting defects', *Eur J Med Genet*, 65: 104456.

Bernassola, F., M. Karin, A. Ciechanover, and G. Melino. 2008. 'The HECT family of E3 ubiquitin ligases: multiple players in cancer development', *Cancer Cell*, 14: 10–21.

Booth, C., K. Masiuk, K. Vazouras, A. Fernandes, J. Xu-Bayford, B. Campo Fernandez, S. Roy, B. Curio-Penny, J. Arnold, D. Terrazas, J. Reid, K. C. Gilmour, S. Adams, E. Alvarez Mediavilla, L. Mhaldien, G. O'Toole, R. Ahmed, E. Garabedian, H. Malech, S. S. De Ravin, T. B. Moore, S. De Oliveira, D. Pellin, T. Y. Lin, T. T. Dang, K. Cornetta, M. S. Hershfield, H. Hara, A. J. Thrasher, H. B. Gaspar, and D. B. Kohn. 2025. 'Long-Term Safety and Efficacy of Gene Therapy for Adenosine Deaminase Deficiency', *N Engl J Med*, 393: 1486–97.

Born, H. A., A. T. Dao, A. T. Levine, W. L. Lee, N. M. Mehta, S. Mehra, E. J. Weeber, and A. E. Anderson. 2017. 'Strain-dependence of the Angelman Syndrome phenotypes in Ube3a maternal deficiency mice', *Sci Rep*, 7: 8451.

Born, H.A., Fetterly, R., Berent, A., Panagoulias, J., Hordeaux, J., Wilson, J.M. 2025. "Nonclinical Efficacy of MVX-220, an AAVhu68-based Investigational Gene Therapy, in a Mouse Model of Angelman Syndrome (AS)." In *European Society of Cell and Gene Therapy*. Seville, Spain

Bronson, S. L., and T. L. Bale. 2016. 'The Placenta as a Mediator of Stress Effects on Neurodevelopmental Reprogramming', *Neuropsychopharmacology*, 41: 207–18.

Buiting, K., B. Dittrich, S. Gross, C. Lich, C. Farber, T. Buchholz, E. Smith, A. Reis, J. Burger, M. M. Nothen, U. Barth-Witte, B. Janssen, D.

Abeliovich, I. Lerer, A. M. van den Ouweland, D. J. Halley, C. Schrander-Stumpel, H. Smeets, P. Meinecke, S. Malcolm, A. Gardner, M. Lalande, R. D. Nicholls, K. Friend, A. Schulze, G. Matthijs, H. Kokkonen, P. Hilbert, L. Van Maldergem, G. Glover, P. Carbonell, P. Willems, G. Gillessen-Kaesbach, and B. Horsthemke. 1998. 'Sporadic imprinting defects in Prader-Willi syndrome and Angelman syndrome: implications for imprint-switch models, genetic counseling, and prenatal diagnosis', *Am J Hum Genet*, 63: 170–80.

Buiting, K., C. Williams, and B. Horsthemke. 2016. 'Angelman syndrome - insights into a rare neurogenetic disorder', *Nat Rev Neurol*, 12: 584–93.

Carson, R. P., L. Bird, A. K. Childers, F. Wheeler, and J. Duis. 2019. 'Preserved expressive language as a phenotypic determinant of Mosaic Angelman Syndrome', *Mol Genet Genomic Med*, 7: e837.

Caruso, A., M. A. Marconi, M. L. Scattoni, and L. Ricceri. 2022. 'Ultrasonic vocalizations in laboratory mice: strain, age, and sex differences', *Genes Brain Behav*, 21: e12815.

Chauhan, M., A. L. Daugherty, F. E. Khadir, O. F. Duzenli, A. Hoffman, J. A. Tinklenberg, P. B. Kang, G. Aslanidi, and C. A. Pacak. 2024. 'AAV-DJ is superior to AAV9 for targeting brain and spinal cord, and de-targeting liver across multiple delivery routes in mice', *J Transl Med*, 22: 824.

Christian, S. L., J. A. Fantes, S. K. Mewborn, B. Huang, and D. H. Ledbetter. 1999. 'Large genomic duplicons map to sites of instability in the Prader-Willi/Angelman syndrome chromosome region (15q11-q13)', *Hum Mol Genet*, 8: 1025–37.

Cooper, E. M., A. W. Hudson, J. Amos, J. Wagstaff, and P. M. Howley. 2004. 'Biochemical analysis of Angelman syndrome-associated mutations in the E3 ubiquitin ligase E6-associated protein', *J Biol Chem*, 279: 41208–17.

Copping, N. A., and J. L. Silverman. 2021. 'Abnormal electrophysiological phenotypes and sleep deficits in a mouse model of Angelman Syndrome', *Mol Autism*, 12: 9.

Crider, K. S., Y. P. Qi, L. F. Yeung, C. T. Mai, L. Head Zauche, A. Wang, K. Daniels, and J. L. Williams. 2022. 'Folic Acid and the Prevention of Birth Defects: 30 Years of Opportunity and Controversies', *Annu Rev Nutr*, 42: 423–52.

Dabrowski, J., A. Czajka, J. Zielinska-Turek, J. Jaroszynski, M. Furtak-Niczyporuk, A. Mela, L. A. Poniatowski, B. Drop, M. Dorobek, M. Barcikowska-Kotowicz, and A. Ziemba. 2019. 'Brain Functional Reserve in the Context of Neuroplasticity after Stroke', *Neural Plast*, 2019: 9708905.

Daily, J. L., K. Nash, U. Jinwal, T. Golde, J. Rogers, M. M. Peters, R. D. Burdine, C. Dickey, J. L. Banko, and E. J. Weeber. 2011. 'Adeno-associated virus-mediated rescue of the cognitive defects in a mouse model for Angelman syndrome', *PLoS One*, 6: e27221.

Dang, H., S. Srinivasa, S. Y. Lee, and C. Alprin. 2023. 'A Case Study of Early Diagnosed Angelman Syndrome: Recognizing Atypical Clinical Presentations', *Cureus*, 15: e39271.

Dehaene-Lambertz, G., and E. S. Spelke. 2015. 'The Infancy of the Human Brain', *Neuron*, 88: 93–109.

Dhungel, B. P., C. G. Bailey, and J. E. J. Rasko. 2021. 'Journey to the Center of the Cell: Tracing the Path of AAV Transduction', *Trends Mol Med*, 27: 172–84.

Dickinson, A. H., M. S. Bowen-Kauth, J. J. Shide, A. E. Youngkin, N. S. Hosamane, C. A. McNair, D. P. Ryan, C. J. Chu, and M. S. Sidorov. 2025. 'Atypical alpha oscillatory EEG dynamics in children with Angelman syndrome', *Neuroimage Clin*, 48: 103865.

Drouyer, M., J. Merjane, T. Nedelkoska, A. Westhaus, S. Scott, S. Lee, P. G. R. Burke, S. McMullan, J. L. Lanciego, A. F. Vicente, R. Bugallo, C. Unzu, G. Gonzalez-Aseguinolaza, A. Gonzalez-Cordero, and L. Lisowski. 2024. 'Enhanced AAV transduction across preclinical CNS models: A comparative study in human brain organoids with cross-species evaluations', *Mol Ther Nucleic Acids*, 35: 102264.

Duncan, C. N., J. R. Bledsoe, B. Grzywacz, A. Beckman, M. Bonner, F. S. Eichler, J. S. Kuhl, M. H. Harris, S. Slauson, R. A. Colvin, V. K. Prasad, G. F. Downey, F. J. Pierciey, M. A. Kinney, M. Foos, A. Lodaya, N. Floro, G. Parsons, A. C. Dietz, A. O. Gupta, P. J. Orchard, H. L. Thakar, and D. A. Williams. 2024. 'Hematologic Cancer after Gene Therapy for Cerebral Adrenoleukodystrophy', *N Engl J Med*, 391: 1287–301.

Fairbrother, L. C., C. Cytrynbaum, P. Boutis, K. Buiting, R. Weksberg, and C. Williams. 2015. 'Mild Angelman syndrome phenotype due to a mosaic methylation imprinting defect', *Am J Med Genet A*, 167: 1565–9.

Filonova, I., J. H. Trotter, J. L. Banko, and E. J. Weeber. 2014. 'Activity-dependent changes in MAPK activation in the Angelman Syndrome mouse model', *Learn Mem*, 21: 98–104.

Frangoul, H., D. Altshuler, M. D. Cappellini, Y. S. Chen, J. Domm, B. K. Eustace, J. Foell, J. de la Fuente, S. Grupp, R. Handgretinger, T. W. Ho, A. Kattamis, A. Kernytsky, J. Lekstrom-Himes, A. M. Li, F. Locatelli, M. Y. Mapara, M. de Montalembert, D. Rondelli, A. Sharma, S. Sheth, S. Soni, M. H. Steinberg, D. Wall, A. Yen, and S. Corbacioglu. 2021. 'CRISPR-Cas9 Gene Editing for Sickle Cell Disease and beta-Thalassemia', *N Engl J Med*, 384: 252–60.

Frohlich, J., M. T. Miller, L. M. Bird, P. Garces, H. Purtell, M. C. Hoener, B. D. Philpot, M. S. Sidorov, W. H. Tan, M. C. Hernandez, A. Rotenberg, S. S. Jeste, M. Krishnan, O. Khwaja, and J. F. Hipp. 2019. 'Electrophysiological Phenotype in Angelman Syndrome Differs Between Genotypes', *Biol Psychiatry*, 85: 752–59.

Fryburg, J. S., W. R. Breg, and V. Lindgren. 1991. 'Diagnosis of Angelman syndrome in infants', *Am J Med Genet*, 38: 58–64.

Galvano, E., H. Pandit, J. Sepulveda, C. A. S. Ng, M. K. Becher, J. S. Mandelblatt, K. Van Dyk, and G. W. Rebeck. 2023. 'Behavioral and transcriptomic effects of the cancer treatment tamoxifen in mice', *Front Neurosci*, 17: 1068334.

Gentile, J. K., W. H. Tan, L. T. Horowitz, C. A. Bacino, S. A. Skinner, R. Barbieri-Welge, A. Bauer-Carlin, A. L. Beaudet, T. J. Bichell, H. S. Lee, T. Sahoo, S. E. Waisbren, L. M. Bird, and S. U. Peters. 2010. 'A neurodevelopmental survey of Angelman syndrome with genotype-phenotype correlations', *J Dev Behav Pediatr*, 31: 592–601.

Gonzalez Ramirez, C., S. G. Salvador, R. K. R. Patel, S. Clark, N. W. Miller, L. M. James, N. W. Ringelberg, J. M. Simon, J. Bennett, D. G. Amaral, A. C. Burette, and B. D. Philpot. 2024. 'Regional and cellular organization of the autism-associated protein UBE3A/E6AP and its antisense transcript in the brain of the developing rhesus monkey', *Front Neuroanat*, 18: 1410791.

Goodspeed, K. 2024. "A GTX-102 Clinical Development Update: Results from the Phase 1/2 Open-label Stuy and an Overview of the Pivotal Phase 3 Study." In *FAST Global Science Summit*

Gooijers, J., L. Pauwels, M. Hehl, C. Seer, K. Cuypers, and S. P. Swinnen. 2024. 'Aging, brain plasticity, and motor learning', *Ageing Res Rev*, 102: 102569.

Grandjean, P., and P. J. Landrigan. 2014. 'Neurobehavioural effects of developmental toxicity', *Lancet Neurol*, 13: 330–8.

Gray, J. T., and S. Zolotukhin. 2011. 'Design and construction of functional AAV vectors', *Methods Mol Biol*, 807: 25–46.

Guoynes, C. D., G. Pavalko, and M. S. Sidorov. 2025. 'Courtship and distress ultrasonic vocalizations are altered in a mouse model of Angelman syndrome', *J Neurodev Disord*, 17: 59.

Hadders-Algra, M. 2018. 'Early human brain development: Starring the subplate', *Neurosci Biobehav Rev*, 92: 276–90.

Hensch, T. K. 2005. 'Critical period plasticity in local cortical circuits', *Nat Rev Neurosci*, 6: 877–88.

Hensch, T. K., and M. Fagiolini. 2005. 'Excitatory-inhibitory balance and critical period plasticity in developing visual cortex', *Prog Brain Res*, 147: 115–24.

Hinderer, C., P. Bell, C. H. Vite, J. P. Louboutin, R. Grant, E. Bote, H. Yu, B. Pukenas, R. Hurst, and J. M. Wilson. 2014. 'Widespread gene transfer in the central nervous system of cynomolgus macaques following delivery of AAV9 into the cisterna magna', *Mol Ther Methods Clin Dev*, 1: 14051.

Hipp, J. F., C. A. Bacino, L. M. Bird, I. Bruenig-Traebert, D. Chan, M. C. de Wit, P. Fontoura, G. Hooper, R. Jagasia, M. L. Krishnan, L. Murtagh, A. Noci, A. R. Martinez, D. Schwab, M. Serrano, M. D. Shen, J. Tillmann, J. Tjeertes, B. Vincenzi, E. Berry-Kravis, A. Bonni, Group Rugonersen Study, and Tangelo investigators all. 2025. 'The UBE3A-ATS antisense oligonucleotide rugonersen in children with Angelman syndrome: a phase 1 trial', *Nat Med*.

Huie, E. Z., X. Yang, M. S. Rioult-Pedotti, M. Naik, Y. A. Huang, J. L. Silverman, and J. Marshall. 2024. 'Peptidomimetic inhibitors targeting TrkB/PSD-95 signaling improves cognition and seizure outcomes in an Angelman Syndrome mouse model', *bioRxiv*.

Huie, E. Z., X. Yang, M. S. Rioult-Pedotti, K. Tran, E. R. Monsen, K. Hansen, M. A. Erickson, M. Naik, A. Y. Yotova, W. A. Banks, Y. A. Huang, J. L. Silverman, and J. Marshall. 2025. 'Peptidomimetic inhibitors targeting TrkB/PSD-95 signaling improves cognition and seizure outcomes in an Angelman Syndrome mouse model', *Neuropsychopharmacology*, 50: 772–82.

Jiang, Y. H., D. Armstrong, U. Albrecht, C. M. Atkins, J. L. Noebels, G. Eichele, J. D. Sweatt, and A. L. Beaudet. 1998. 'Mutation of the Angelman ubiquitin ligase in mice causes increased cytoplasmic p53 and deficits of contextual learning and long-term potentiation', *Neuron*, 21: 799–811.

Jiang, Y. H., Y. Pan, L. Zhu, L. Landa, J. Yoo, C. Spencer, I. Lorenzo, M. Brilliant, J. Noebels, and A. L. Beaudet. 2010. 'Altered ultrasonic vocalization and impaired learning and memory in Angelman syndrome mouse model with a large maternal deletion from Ube3a to Gabrb3', *PLoS One*, 5: e12278.

Jiang, Y., Zhou, J. 2024 "Non-Viral Gene Editing for Angelman Syndrome: Progress and Updates " In *FAST Global Science Summit* Orlando FL.

Judson, M. C., C. Shyng, J. M. Simon, C. R. Davis, A. M. Punt, M. T. Salmon, N. W. Miller, K. D. Ritola, Y. Elgersma, D. G. Amaral, S. J. Gray, and B. D. Philpot. 2021. 'Dual-isoform hUBE3A gene transfer improves behavioral and seizure outcomes in Angelman syndrome model mice', *JCI Insight*, 6.

Judson, M. C., M. L. Wallace, M. S. Sidorov, A. C. Burette, B. Gu, G. M. van Woerden, I. F. King, J. E. Han, M. J. Zylka, Y. Elgersma, R. J. Weinberg, and B. D. Philpot. 2016. 'GABAergic Neuron-Specific Loss of Ube3a Causes Angelman Syndrome-Like EEG Abnormalities and Enhances Seizure Susceptibility', *Neuron*, 90: 56–69.

Keute, M., M. T. Miller, M. L. Krishnan, A. Sadhwani, S. Chamberlain, R. L. Thibert, W. H. Tan, L. M. Bird, and J. F. Hipp. 2021. 'Angelman syndrome genotypes manifest varying degrees of clinical severity and developmental impairment', *Mol Psychiatry*, 26: 3625–33.

Khan, N., R. Cabo, W. H. Tan, R. Tayag, and L. M. Bird. 2019. 'An observational study of pediatric healthcare burden in Angelman syndrome: results from a real-world study', *Orphanet J Rare Dis*, 14: 239.

Kishino, T., M. Lalande, and J. Wagstaff. 1997. 'UBE3A/E6-AP mutations cause Angelman syndrome', *Nat Genet*, 15: 70–3.

Knudsen, E. I. 2004. 'Sensitive periods in the development of the brain and behavior', *J Cogn Neurosci*, 16: 1412–25.

Kuhl, P. K., and A. N. Meltzoff. 1996. 'Infant vocalizations in response to speech: vocal imitation and developmental change', *J Acoust Soc Am*, 100: 2425–38.

La Manno, G., K. Siletti, A. Furlan, D. Gyllborg, E. Vinsland, A. Mossi Albiach, C. Mattsson Langseth, I. Khven, A. R. Lederer, L. M. Dratva, A. Johnsson, M. Nilsson, P. Lonnerberg, and S. Linnarsson. 2021. 'Molecular architecture of the developing mouse brain', *Nature*, 596: 92–96.

Lauer, A., S. L. Speroni, M. Choi, X. Da, C. Duncan, S. McCarthy, V. Krishnan, C. A. Lusk, D. Rohde, M. B. Hansen, J. Kalpathy-Cramer, D. J. Loes, P. A. Caruso, D. A. Williams, K. Mouridsen, K. E. Emblem, F. S. Eichler, and P. L. Musolino. 2023. 'Hematopoietic stem-cell gene therapy is associated with restored white matter microvascular function in cerebral adrenoleukodystrophy', *Nat Commun*, 14: 1900.

Lee, D., W. Chen, H. N. Kaku, X. Zhuo, E. S. Chao, A. Soriano, A. Kuncheria, S. Flores, J. H. Kim, A. Rivera, F. Rigo, P. Jafar-Nejad, A. L. Beaudet, M. S. Caudill, and M. Xue. 2023. 'Antisense oligonucleotide therapy rescues disturbed brain rhythms and sleep in juvenile and adult mouse models of Angelman syndrome', *Elife*, 12.

Li, X., Z. J. Du, M. Q. Chen, J. J. Chen, Z. M. Liang, X. T. Ding, M. Zhou, S. J. Li, X. W. Li, J. M. Yang, and T. M. Gao. 2020. 'The effects of tamoxifen on mouse behavior', *Genes Brain Behav*, 19: e12620.

Liguore, W. A., J. S. Domire, D. Button, Y. Wang, B. D. Dufour, S. Srinivasan, and J. L. McBride. 2019. 'AAV-PHP.B Administration Results in a Differential Pattern of CNS Biodistribution in Non-human Primates Compared with Mice', *Mol Ther*, 27: 2018–37.

Lossie, A. C., M. M. Whitney, D. Amidon, H. J. Dong, P. Chen, D. Theriaque, A. Hutson, R. D. Nicholls, R. T. Zori, C. A. Williams, and D. J. Driscoll. 2001. 'Distinct phenotypes distinguish the molecular classes of Angelman syndrome', *J Med Genet*, 38: 834–45.

Lu, X. . 2023. "The Novel Large Deletion Mouse Model of AS: How Can it Help us in Drug Development for Angelman Syndrome?" In *2023 FAST Summit on Angelman Syndrome* Orlando FL.

Lu, X. 2025. "Brain-wide Genome Editing via STEP-RNPs for Treatment of Angelman Syndrome." In *American Society of Cell and Gene Therapy Annual Meeting*. New Orleans LA

Luthers, C. 2025. "Hematopoietic Stem Cell Lentiviral Gene Therapy for the Treatment of Angelman Syndrome." In *American Society of Cell and Gene Therapy*. New Orleans LA

Lutter, C. K., J. P. Pena-Rosas, and R. Perez-Escamilla. 2013. 'Maternal and child nutrition', *Lancet*, 382: 1550–1.

Margolis, S. S., G. L. Sell, M. A. Zbinden, and L. M. Bird. 2015. 'Angelman Syndrome', *Neurotherapeutics*, 12: 641–50.

Martinez, L. A., H. A. Born, S. Harris, A. Regnier-Golanov, J. C. Grieco, E. J. Weeber, and A. E. Anderson. 2023. 'Quantitative EEG Analysis in Angelman Syndrome: Candidate Method for Assessing Therapeutics', *Clin EEG Neurosci*, 54: 203–12.

Mathiesen, S. N., J. L. Lock, L. Schoderboeck, W. C. Abraham, and S. M. Hughes. 2020. 'CNS Transduction Benefits of AAV-PHP.eB over AAV9 Are Dependent on Administration Route and Mouse Strain', *Mol Ther Methods Clin Dev*, 19: 447–58.

Matsuura, T., J. S. Sutcliffe, P. Fang, R. J. Galjaard, Y. H. Jiang, C. S. Benton, J. M. Rommens, and A. L. Beaudet. 1997. 'De novo truncating mutations in E6-AP ubiquitin-protein ligase gene (UBE3A) in Angelman syndrome', *Nat Genet*, 15: 74–7.

Meng, L., R. E. Person, and A. L. Beaudet. 2012. 'Ube3a-ATS is an atypical RNA polymerase II transcript that represses the paternal expression of Ube3a', *Hum Mol Genet*, 21: 3001–12.

Meng, L., A. J. Ward, S. Chun, C. F. Bennett, A. L. Beaudet, and F. Rigo. 2015. 'Towards a therapy for Angelman syndrome by targeting a long non-coding RNA', *Nature*, 518: 409–12.

Milazzo, C., E. J. Mientjes, I. Wallaard, S. V. Rasmussen, K. D. Erichsen, T. Kakunuri, A. S. E. van der Sman, T. Kremer, M. T. Miller, M. C. Hoener, and Y. Elgersma. 2021. 'Antisense oligonucleotide treatment rescues UBE3A expression and multiple phenotypes of an Angelman syndrome mouse model', *JCI Insight*, 6.

Mishra, A., and N. R. Jana. 2008. 'Regulation of turnover of tumor suppressor p53 and cell growth by E6-AP, a ubiquitin protein ligase mutated in Angelman mental retardation syndrome', *Cell Mol Life Sci*, 65: 656–66.

Miura, K., T. Kishino, E. Li, H. Webber, P. Dikkes, G. L. Holmes, and J. Wagstaff. 2002. 'Neurobehavioral and electroencephalographic abnormalities in Ube3a maternal-deficient mice', *Neurobiol Dis*, 9: 149–59.

Moxley, J., J. Sharit, and S. J. Czaja. 2022. 'The Factors Influencing Older Adults' Decisions Surrounding Adoption of Technology: Quantitative Experimental Study', *JMIR Aging*, 5: e39890.

Nawaz, Z., D. M. Lonard, C. L. Smith, E. Lev-Lehman, S. Y. Tsai, M. J. Tsai, and B. W. O'Malley. 1999. 'The Angelman syndrome-associated protein, E6-AP, is a coactivator for the nuclear hormone receptor superfamily', *Mol Cell Biol*, 19: 1182–9.

Nazlican, H., M. Zeschnigk, U. Claussen, S. Michel, S. Boehringer, G. Gillessen-Kaesbach, K. Buiting, and B. Horsthemke. 2004. 'Somatic mosaicism in patients with Angelman syndrome and an imprinting defect', *Hum Mol Genet*, 13: 2547–55.

Nenninger, A. W., M. Willman, J. Willman, E. Stewart, P. Mesidor, M. Novoa, N. K. Morrill, L. Alvarez, A. Joly-Amado, M. M. Peters, D. Gulick, and K. R. Nash. 2022. 'Improving Gene Therapy for Angelman Syndrome with Secreted Human UBE3A', *Neurotherapeutics*, 19: 1329–39.

O'Geen, H., U. Beitnere, M. S. Garcia, A. Adhikari, D. L. Cameron, T. A. Fenton, N. A. Copping, P. Deng, S. Lock, Janm Halmai, I. J. Villegas, J. Liu, D. Wang, K. D. Fink, J. L. Silverman, and D. J. Segal. 2023. 'Transcriptional reprogramming restores UBE3A brain-wide and rescues behavioral phenotypes in an Angelman syndrome mouse model', *Mol Ther*, 31: 1088–105.

Parenti, I., L. G. Rabaneda, H. Schoen, and G. Novarino. 2020. 'Neurodevelopmental Disorders: From Genetics to Functional Pathways', *Trends Neurosci*, 43: 608–21.

Pauwels, L., S. Chalavi, and S. P. Swinnen. 2018. 'Aging and brain plasticity', *Aging (Albany NY)*, 10: 1789–90.

Pearson, E., L. Wilde, M. Heald, R. Royston, and C. Oliver. 2019. 'Communication in Angelman syndrome: a scoping review', *Dev Med Child Neurol*, 61: 1266–74.

Pranic, N. M., C. Kornbrek, C. Yang, T. A. Cleland, and K. A. Tschida. 2022. 'Rates of ultrasonic vocalizations are more strongly related than acoustic features to non-vocal behaviors in mouse pups', *Front Behav Neurosci*, 16: 1015484.

Punatar, R., A. Egense, R. Mao, M. Procter, M. Bosworth, D. I. Quigley, K. Angkustsiri, and S. P. Shankar. 2022. 'Atypical presentation of Angelman syndrome with intact expressive language due to low-level mosaicism', *Mol Genet Genomic Med*, 10: e2018.

Rauh, V. A., and A. E. Margolis. 2016. 'Research Review: Environmental exposures, neurodevelopment, and child mental health - new paradigms for the study of brain and behavioral effects', *J Child Psychol Psychiatry*, 57: 775–93.

Reed, S., R. Shell, K. Kassis, K. Tartaglia, R. Wallihan, K. Smith, L. Hurtubise, B. Martin, C. Ledford, S. Bradbury, H. H. Bernstein, and J. D. Mahan. 2014. 'Applying adult learning practices in medical education', *Curr Probl Pediatr Adolesc Health Care*, 44: 170–81.

Riedel, A., C. Faul, K. Reuss, J. C. Schroder, P. J. Lang, C. Lengerke, N. Weissert, H. Hengel, S. Groschel, L. Schoels, and W. A. Bethge. 2024. 'Allogeneic hematopoietic cell transplantation for adult metachromatic leukodystrophy: a case series', *Blood Adv*, 8: 1504–08.

Rockwell, B., P. Ramamurthy, J. A. Verceles, A. Lombardo, A. Verma, and D. L. Cooper. 2025. 'Hematopoietic Stem Cell Transplant in Adult Patients with Fanconi Anemia: A Review', *Diseases*, 13.

Rougeulle, C., and M. Lalande. 1998. 'Angelman syndrome: how many genes to remain silent?', *Neurogenetics*, 1: 229–37.

Sadhwani, A., S. Powers, A. Wheeler, H. Miller, S. N. Potter, S. U. Peters, C. A. Bacino, S. A. Skinner, L. K. Wink, C. A. Erickson, L. M. Bird, and W. H. Tan. 2024. 'Developmental milestones and daily living skills in individuals with Angelman syndrome', *J Neurodev Disord*, 16: 32.

Sadhwani, A., A. Wheeler, A. Gwaltney, S. U. Peters, R. L. Barbieri-Welge, L. T. Horowitz, L. M. Noll, R. J. Hundley, L. M. Bird, and W. H. Tan. 2023. 'Developmental Skills of Individuals with Angelman Syndrome Assessed Using the Bayley-III', *J Autism Dev Disord*, 53: 720–37.

Scheffner, M., U. Nuber, and J. M. Huibregtse. 1995. 'Protein ubiquitination involving an E1-E2-E3 enzyme ubiquitin thioester cascade', *Nature*, 373: 81–3.

Schmid, R. S., X. Deng, P. Panikker, M. Msackyi, C. Breton, and J. M. Wilson. 2021. 'CRISPR/Cas9 directed to the Ube3a antisense transcript improves Angelman syndrome phenotype in mice', *J Clin Invest*, 131.

Semple, B. D., K. Blomgren, K. Gimlin, D. M. Ferriero, and L. J. Noble-Haeusslein. 2013. 'Brain development in rodents and humans: Identifying benchmarks of maturation and vulnerability to injury across species', *Prog Neurobiol*, 106-107: 1–16.

Sharit, J., and S. J. Czaja. 2020. 'Overcoming Older Adult Barriers to Learning Through an Understanding of Perspectives on Human Information Processing', *J Appl Gerontol*, 39: 233–41.

Sidorov, M. S., G. M. Deck, M. Dolatshahi, R. L. Thibert, L. M. Bird, C. J. Chu, and B. D. Philpot. 2017. 'Delta rhythmicity is a reliable EEG biomarker in Angelman syndrome: a parallel mouse and human analysis', *J Neurodev Disord*, 9: 17.

Silva-Santos, S., G. M. van Woerden, C. F. Bruinsma, E. Mientjes, M. A. Jolfaei, B. Distel, S. A. Kushner, and Y. Elgersma. 2015. 'Ube3a reinstatement identifies distinct developmental windows in a murine Angelman syndrome model', *J Clin Invest*, 125: 2069–76.

Syding, L. A., A. Kubik-Zahorodna, P. Nickl, V. Novosadova, J. Kopkanova, P. Kasparek, J. Prochazka, and R. Sedlacek. 2022. 'Generation and Characterization of a Novel Angelman Syndrome Mouse Model with a Full Deletion of the Ube3a Gene', *Cells*, 11.

Tandon, P. K., and E. D. Kakkis. 2021. 'The multi-domain responder index: a novel analysis tool to capture a broader assessment of clinical benefit in heterogeneous complex rare diseases', *Orphanet J Rare Dis*, 16: 183.

Thomason, M. E., and C. L. Hendrix. 2024. 'Prenatal Stress and Maternal Role in Neurodevelopment', *Annu Rev Dev Psychol*, 6: 87–107.

Thomason, M. E., A. C. Palopoli, N. N. Jariwala, D. M. Werchan, A. Chen, S. Adhikari, C. Espinoza-Heredia, N. H. Brito, and C. J. Trentacosta. 2021. 'Miswiring the brain: Human prenatal Delta9-tetrahydrocannabinol use associated with altered fetal hippocampal brain network connectivity', *Dev Cogn Neurosci*, 51: 101000.

Tomaic, V., and L. Banks. 2015. 'Angelman syndrome-associated ubiquitin ligase UBE3A/E6AP mutants interfere with the proteolytic activity of the proteasome', *Cell Death Dis*, 6: e1625.

van Woerden, G. M., K. D. Harris, M. R. Hojjati, R. M. Gustin, S. Qiu, R. de Avila Freire, Y. H. Jiang, Y. Elgersma, and E. J. Weeber. 2007. 'Rescue of neurological deficits in a mouse model for Angelman syndrome by reduction of alphaCaMKII inhibitory phosphorylation', *Nat Neurosci*, 10: 280–2.

Wagstaff, J., J. H. Knoll, K. A. Glatt, Y. Y. Shugart, A. Sommer, and M. Lalande. 1992. 'Maternal but not paternal transmission of 15q11-13-linked nondeletion Angelman syndrome leads to phenotypic expression', *Nat Genet*, 1: 291–4.

Wang, J. H., D. J. Gessler, W. Zhan, T. L. Gallagher, and G. Gao. 2024. 'Adeno-associated virus as a delivery vector for gene therapy of human diseases', *Signal Transduct Target Ther*, 9: 78.

Weeber, E. J., Y. H. Jiang, Y. Elgersma, A. W. Varga, Y. Carrasquillo, S. E. Brown, J. M. Christian, B. Mirnikjoo, A. Silva, A. L. Beaudet, and J. D. Sweatt. 2003. 'Derangements of hippocampal calcium/calmodulin-dependent protein kinase II in a mouse model for Angelman mental retardation syndrome', *J Neurosci*, 23: 2634–44.

Werwach, A., D. Murbe, G. Schaadt, and C. Mannel. 2021. 'Infants' vocalizations at 6 months predict their productive vocabulary at one year', *Infant Behav Dev*, 64: 101588.

Wheeler, A. C., P. Sacco, and R. Cabo. 2017. 'Unmet clinical needs and burden in Angelman syndrome: a review of the literature', *Orphanet J Rare Dis*, 12: 164.

Williams, C. A., D. J. Driscoll, and A. I. Dagli. 2010. 'Clinical and genetic aspects of Angelman syndrome', *Genet Med*, 12: 385–95.

Wolter, J. M., H. Mao, G. Fragola, J. M. Simon, J. L. Krantz, H. O. Bazick, B. Oztemiz, J. L. Stein, and M. J. Zylka. 2020. 'Cas9 gene therapy for Angelman syndrome traps Ube3a-ATS long non-coding RNA', *Nature*, 587: 281–84.

Yang, X., and Y. A. Huang. 2025. 'Unraveling the Roles of UBE3A in Neurodevelopment and Neurodegeneration', *Int J Mol Sci*, 26.

Zori, R. T., J. Hendrickson, S. Woolven, E. M. Whidden, B. Gray, and C. A. Williams. 1992. 'Angelman syndrome: clinical profile', *J Child Neurol*, 7: 270–80.

Zotey, V., A. Andhale, T. Shegekar, and A. Juganavar. 2023. 'Adaptive Neuroplasticity in Brain Injury Recovery: Strategies and Insights', *Cureus*, 15: e45873.